UNIVERSIDADE FEDERAL DE SÃO CARLOS
CENTRO DE CIÊNCIAS EXATAS E DE TECNOLOGIA
DEPARTAMENTO DE QUÍMICA
PROGRAMA DE PÓS-GRADUAÇÃO EM QUÍMICA

"DESENVOLVIMENTO DE PROCEDIMENTOS DE PREPARO DE AMOSTRAS DE DIFÍCIL MINERALIZAÇÃO PARA ANÁLISE DIRETA POR LASER-INDUCED BREAKDOWN SPECTROSCOPY (LIBS)"

Marco Aurelio Sperança*

Tese apresentada como parte dos requisitos para obtenção do título de DOUTOR EM CIÊNCIAS, área de concentração: QUÍMICA ANALÍTICA

Orientador(a): Prof. Dr. Edenir Rodrigues Pereira Filho

* bolsista CNPq (processo nº 160152/2015-1)

São Carlos - SP
2019

UNIVERSIDADE FEDERAL DE SÃO CARLOS

Centro de Ciências Exatas e de Tecnologia
Programa de Pós-Graduação em Química

Folha de Aprovação

Assinaturas dos membros da comissão examinadora que avaliou e aprovou a Defesa de Tese de Doutorado do candidato Marco Aurelio Sperança, realizada em 27/08/2019:

Prof. Dr. Edenir Rodrigues Pereira Filho
UFSCar

Prof. Dr. Manoel Gustavo Petrucelli Homem
UFSCar

Profa. Dra. Heloisa França Maltez
UFABC

Prof. Dr. Jader de Souza Cabral
UFU

Prof. Dr. Pedro Sergio Fadini
UFSCar

"Tudo posso naquele que me fortalece"

Filipenses 4:13

Dedico este trabalho a minha esposa Gabriela e filha Elisa.
Também dedico aos meus pais José Maria e Nelcy
e aos meus irmãos Ana Carolina e Hugo Leonardo.

Agradeço primeiramente a Deus por me abençoar com saúde, energia e discernimento para conclusão deste trabalho de tese.

Agradeço também a minha esposa por ser mais companheira do que eu poderia imaginar ou querer, estando sempre ao meu lado em todos os momentos, bons ou ruins e também por me dar meu maior presente, a Elisa. Agradeço também a vida dela, que me fez entender o amor de uma maneira incondicional. Elas são o motivo pelo qual eu lutei, luto e lutarei pelo resto da minha vida.

Agradeço aos meus maiores exemplos de vida, meu pai e minha mãe, pela criação maravilhosa com princípios e valores que todo ser humano deveria conhecer, pelo amor demonstrado de várias formas, pelo cuidado e preocupação com a vida dos três filhos e por terem nos incentivado a sermos pessoas melhores que eles.

Agradeço ao meu irmão e à minha irmã por serem meus maiores companheiros e também grandes exemplos de pessoas, por serem 7 e 9 anos mais velhos, respectivamente.

Agradeço aos meus pais e irmãos por mostrarem como deve ser uma família de verdade, onde há honestidade, companheirismo, vitórias, derrotas, alegrias, tristezas, disciplina e o mais importante, o amor.

Agradeço ao meu orientador, Prof. Edenir, por ter sido um exemplo de profissional durante todos os 6 anos de convivência que tivemos, pela orientação excelente ao longo do meu mestrado e doutorado e pela amizade que com certeza levarei para onde quer que eu vá. Uma excelente pessoa, e também um dos exemplos que me forjaram como eu sou hoje.

Agradeço ao professor Joaquim e à pesquisadora Ana Rita pela colaboração em todas as etapas do meu doutorado

This PhD thesis is based on the following publications and manuscript for publication, which are presented in the original format:

"Analysis of Cuban nickeliferous minerals by laser-induced breakdown spectroscopy (LIBS): non-conventional sample preparation of powder samples"

Marco Aurelio Sperança, Mario Siméon Pomares-Alfonso, Edenir Rodrigues Pereira-Filho. *Analytical Methods* 10 (2018) 533-540.

"Determination of Elemental Content in Solder Mask Samples Used in Printed Circuit Boards Using Different Spectroanalytical Techniques"

Marco Aurelio Sperança, Alex Virgilio, Edenir Rodrigues Pereira-Filho, Francisco Wendel Batista de Aquino. *Applied Spectroscopy* 72(8) (2018) 1205-1214.

"Univariate and multivariate calibration strategies in combination with laser-induced breakdown spectroscopy (LIBS) to determine Ti on sunscreen: A different sample preparation procedure"

Marco Aurelio Sperança, Daniel Fernandes Andrade, Jeyne Pricylla Castro, Edenir Rodrigues Pereira-Filho. *Optics and Laser Technology* 109 (2019) 648-653.

LIST OF ACRONYMS

DoE – Design of experiments

EDTA – Ethylenediamine tetraacetic acid

ICP OES – Inductively coupled plasma optical emission spectrometry

ICP-MS – Inductively coupled plasma – mass spectrometry

KNN – k-Nearest neighbor

LDA – Linear discriminant analysis

LIBS – Laser-induced breakdown spectroscopy

LOD – Limit of detection

MLR – Multiple linear regression

PCA – Principal component analysis

PCB – Printed circuit board

PCR – Principal component regression

PLS – Partial least square

PLS DA – Partial least square discriminant analysis

PVA – Polyvinyl alcohol

SECV – Standard error of cross-validation

SEV – Standard error of validation

SIMCA – Soft independent modeling of class analogy

SPF – Sun protection factor

SRM – Surface response methodology

UV – Ultraviolet radiation

UVA – Ultraviolet radiation A

UVB – Ultraviolet radiation B

LIST OF FIGURES

RESUMO

DESENVOLVIMENTO DE PROCEDIMENTOS DE PREPARO DE AMOSTRAS DE DIFÍCIL MINERALIZAÇÃO PARA ANÁLISE DIRETA POR LASER-INDUCED BREAKDOWN SPECTROSCOPY (LIBS). Esta tese de doutorado propõe preparos de amostra aliados a utilização da técnica espectroanalítica de emissão atômica induzida por laser (*laser-induced breakdown spectroscopy, LIBS*) para análise de amostras de difícil mineralização com foco no desenvolvimento analítico da LIBS bem como para o desenvolvimento de preparo de amostras para a técnica. A técnica LIBS consiste na focalização de um pulso de laser com alta fluência (> GW s^{-1}) sob a superfície de uma amostra. Após a incidência desse laser, os átomos são vaporizados, atomizados, ionizados e levados a um estado de energia excitado. Quando átomos e íons retornam aos seus níveis energéticos mais baixos liberam fótons com comprimentos de onda específicos que são traduzidos em espectro eletromagnético. A técnica possui desafios inerentes à análise de amostras sólidas, que são majoritariamente suas aplicações, como microheterogeneidade e altos limites de detecção (LOD). Apesar da técnica possuir grande habilidade na análise de amostras sólidas, pode também ser usada para análise de amostras líquidas, no entanto, alguns problemas específicos surgem, como espalhamento da amostra com o impacto do pulso de laser e baixa reprodutibilidade, e o preparo das amostras pode ajudar a minimizá-los. Como objetivo, a presente tese se concentra no desenvolvimento de preparo de amostras de minério de níquel, máscara de solda e protetores solares para análise de elementos de interesse em cada uma das amostras apresentadas. A estratégia para análise de amostras de minério de níquel e protetor solar consistiu na conversão da matriz de líquido para sólido no intuito de minimizar os problemas inerentes à análise de líquidos por LIBS, para isso, álcool poli vinílico (PVA), polímero hidrossolúvel, foi utilizado. Para máscaras de solda, as amostras foram totalmente secas em suporte de vidro para posterior análise. Ferramentas quimiométricas foram utilizadas durante o trabalho para auxílio do tratamento de dados (normalizações), análise exploratória (PCA (*principal component analysis*)) e calibração uni e multivariada (PCR (*principal component regression*), PLS (*partial least squares*), MLR (*multiple linear regression*)).

ABSTRACT

DEVELOPMENT OF SAMPLE PREPARATION PROCEDURES FOR DIFFICULT-TO-MINERALIZE SAMPLES FOR DIRECT ANALYSIS BY LASER-INDUCED BREAKDOWN SPECTROSCOPY (LIBS). This doctoral thesis proposes sample preparation combined with the use of laser-induced breakdown spectroscopy (LIBS) for analysis of difficult-to-mineralize samples focusing on the analytical development of LIBS as well as for the development of sample preparation for the technique. The LIBS technique consists of focusing a laser pulse with high fluence (> GW s-1) under the surface of a sample. Following the incidence of this laser pulse, atoms are vaporized, atomized, ionized and brought into an excited energy state. When atoms and ions return to their lowest energy levels, they release photons of specific wavelengths that are translated into the electromagnetic spectrum. The technique has inherent challenges in the analysis of solid samples, which are mostly its applications, such as microheterogeneity and high limits of detection (LOD). Although the technique has great ability in solid sample analysis, it can also be used for liquid sample analysis, however, some specific problems arise, such as sample splashing with laser pulse impact and low reproducibility, and sample preparation can help minimize them. As goal, the present thesis focuses on the development of sample preparation of nickel ores, solder masks and sunscreens for analysis of elements of interest in each of the presented samples. The strategy for the analysis of nickel ore and sunscreen samples consisted of converting the matrix of liquid to solid in order to minimize the problems inherent to liquid analysis by LIBS. For this, polyvinyl alcohol (PVA), a water-soluble polymer, was used. For solder masks, the samples were completely dried on glass support for further analysis. Chemometric tools were used during the work to aid in data processing (normalization), exploratory analysis (PCA (principal component analysis)) and univariate and multivariate calibration (PCR (principal component regression), PLS (partial least squares), MLR (multiple linear regression)).

SUMMARY

Chapter 1 – Introduction

1.1. Introduction

The search of analytical techniques that fits perfectly for specific analytical problems have arisen over the last decades due the need of saving time and resources and diminishing the consumption of reagents and the residue generation. In this context, materials such as mineral ores are usually a tough material, with high economic importance (e.g. nickeliferous minerals for Cuba), and difficult to mineralize for wet-based determinations of elements of interest [1-3]. In order to perform these determinations, a prior sample preparation step is required due to the wet-based feature of the instruments used. Usually, inductively coupled plasma (ICP) optical emission spectrometry (OES) and ICP-mass spectrometry (MS) are employed [4]. The sample preparation for this type of samples usually consists on microwave-assisted mineralization using strong acids or combination of them, or fusion techniques which brings reliable, but unsafe, laborious and time-consuming procedures [2].

Solder masks are materials used in the production of printed-circuit boards (PCB). They are important because are responsible for some properties on the PCB, such as: 1) coating; 2) insulation; and 3) mechanical resistance [5-6]. Regarding health issues, allergenic reports are related in the literature [7], thus, requiring special attention related to their quality control, especially regarding the elemental composition of this material [8]. Sample preparation for this type of samples usually needs two steps due to the presence of $BaSO_4$, insoluble compound responsible for some features in this material [9-10]. After a microwave acid mineralization employing strong acids under high pressure and temperature, a dissolution of the precipitated with ethylenediamine tetraacetic acid

(EDTA) on basic pH and heating is needed [8]. This second step is needed to determine Ba in these samples ($BaSO_4$ insoluble in HNO_3).

Sunscreens are lotions intended to prevent skin damages through the absorption and/or scattering of ultraviolet radiation (UV) A (320 – 400 nm) and UVB (290 – 320 nm) [11]. Inorganic (e.g. TiO_2) and organic (benzophenone) filters are used for these tasks in sunscreen formulation. Focusing on the inorganic filter TiO_2, the concentration of this compound is correlated with the sun protection factor (SPF) of the sunscreen and must be assessed to guarantee quality of this material. For wet-based determinations, the sample preparation inevitably passes through the use of HF acid due to the insolubility of the compound on HNO_3 [12].

In this context, laser-based plasma techniques such as laser-induced breakdown spectroscopy (LIBS) have arisen considerably on analytical applications over the last decades due to some features that will be discussed in the next section.

1.2. Laser-induced breakdown spectroscopy (LIBS)

Laser-induced breakdown spectroscopy (LIBS) is a emission plasma-based technique that employs laser pulses on the surface of a material that can be solid, liquid, or on gaseous samples. This laser pulse, with high fluence (> GW s^{-1}) generates plasma that reaches high temperatures (~50000 K in the beginning) which is enough to vaporize, atomize and ionize the elements on the region hit by the laser. The atoms and ions then go to a higher energy level, and when they come back for lower energy levels, emit photons with specific energies that is further traduced on emission spectra [13-16].

The specialized literature (Web of Science® online database) reports 4611 studies on the search for "laser-induced breakdown spectroscopy" since 1981. On FIGURE 1.2.1 it is possible to see the evolution of the number of researches developed over the years. This noteworthy increasing in the studies number over the years after 1995 are due to technological advances on pulsed laser and stabilization of electronics development, and also to the feasibility of the technique in overcome a whole variety of applications on the analytical chemistry [17].
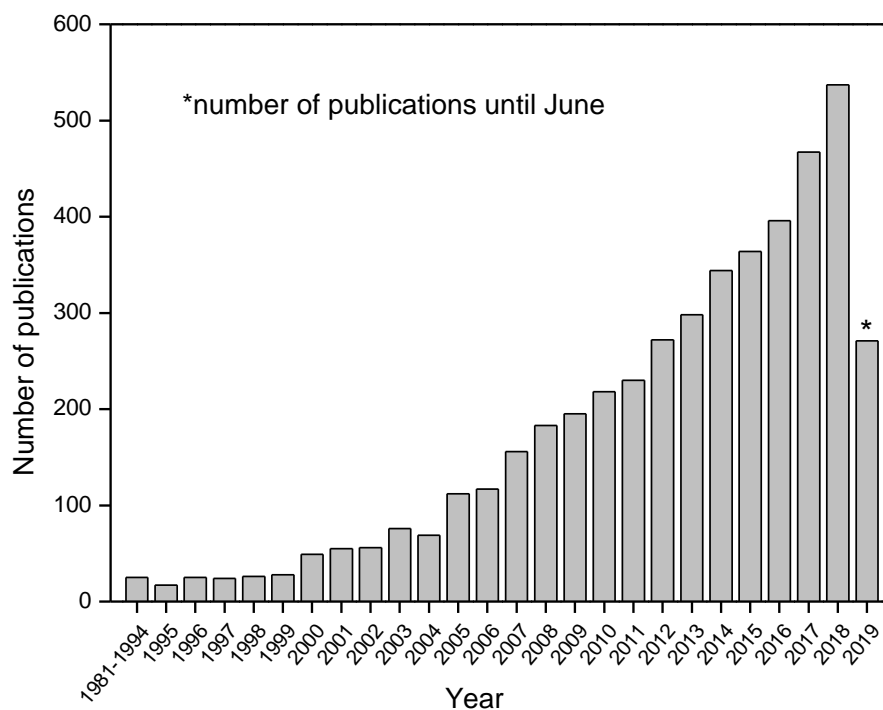
FIGURE 1.2.1 – Number of publications over the years about "laser-induced breakdown spectroscopy" (Web of Science® online database).

Regarding liquid sample analysis, over a hundred studies are found in the literature and the evolution of the production over the years can be seen on FIGURE 1.2.2.

It is possible to note that the profile of publications varies over the years probably due to the difficult of this type of applications (LIBS is mostly used for solid sample analysis).
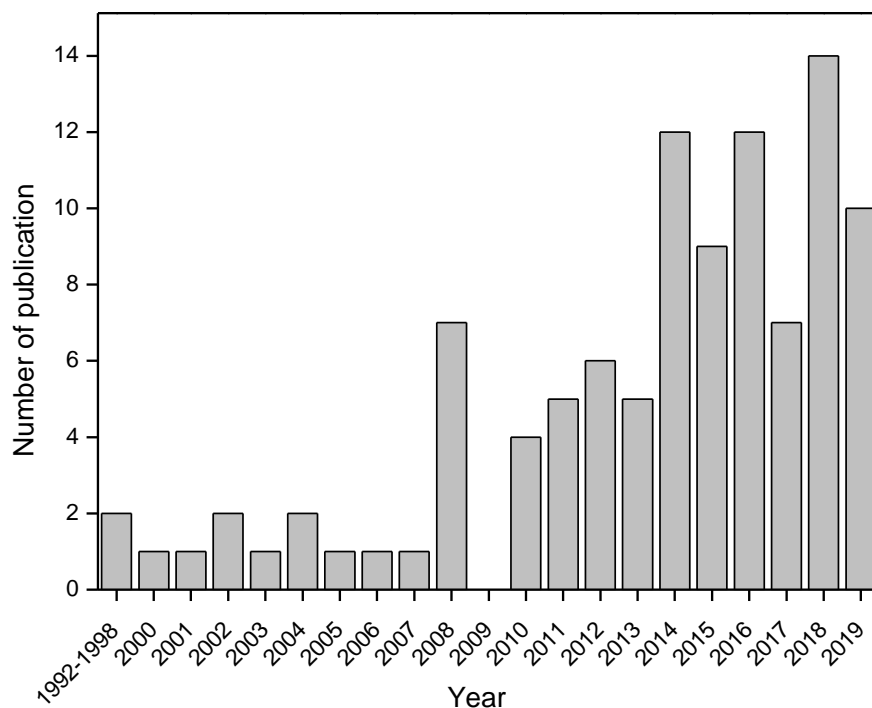
FIGURE 1.2.2 - Number of publications over the years about "laser-induced breakdown spectroscopy" AND "liquid samples" (Web of Science® online database).

With the information derived from FIGURE 1.2.1 and FIGURE 1.2.2, it is possible to see that the LIBS technique is evolving through time, but it is still a challenge to analyze liquid samples by LIBS. Although LIBS is mainly used to analyze solid samples, there is a few analytical applications in liquid samples that could be overcome using LIBS, hence, lacking of appropriate methodologies. Some viscous and liquid samples have high concentration levels of elements of interest, in this case, being LIBS a feasible technique to perform this analysis.

1.3. Sample preparation for LIBS analysis

One of the most attractive features of LIBS technique is the possibility of direct analysis with minimal or no sample preparation [18,19]. Despite the technique is mostly used for solid sample analysis, it has the possibility of analyzing samples in liquid and gaseous forms, showing flexibility. This section is responsible to bring the main sample preparation strategies, advantages and challenges for LIBS analysis of solid, and liquid samples.

Commonly, the solid samples can be directly analyzed, in their natural form [20] and in the form of pellets prepared from the ground and/or milled material [19]. For solid samples having appropriate homogeneity, grounding and/or milling steps can be avoided, such as glass samples [21], metal alloys [22], polymers [23], fossils [24] and orthopedic alloys [25]. It is important to note that the homogeneity of the mentioned samples come from their original constitution, and therefore the preparation step is dispensed.

For heterogeneous solid samples, a grinding step is recommended in order to reduce particle size. This step is important, as it aims to reduce the heterogeneity of the samples, providing high reproducibility analysis. After this step, now with the homogeneous samples in the form of powder, pressing this material in the form of pellets is recommended [19]. Concerning the mass of the sample used to prepare the pellets, factors such as the diameter, thickness required and the density of the material should be evaluated. For example, for cattle mineral supplement tablets with a diameter of 12 mm and a thickness of 3 mm, 500 mg of sample is required [26]. In the preparation of pellets, it should be ensured that they are cohesive and resistant to withstand the shockwave

during the expansion of the plasma induced by the laser pulse. The cohesion and strength of the pellets are directly linked to the particle size distribution. In the case of vegetable material pellets, it is recommended that the particles be less than 100 μm. In general, the pellets prepared with smaller particles are more resistant, and this directly reflects on the precision of the measurements, because the more compact and mechanically resistant the pellet is the more reproducible the interaction between the laser and the sample [19].

Although pressing the materials into pellets is very simple, in some cases it is not possible to produce tablets for some samples that are in powder form. Thus, it is recommended to use a binder material to minimize differences in porosity, ensuring greater strength and efficiency in laser-matter interaction. Some types of binders have been used for the preparation of pellets, for example microcrystalline cellulose. The ratio of binder/sample mass in the pellet preparation may range from 10 to 50%, and this variation depends on factors such as sample properties and the mechanical strength of the pellets [19]. In the proposed study by Peruchi et al. [27] the authors have analyzed wheat flour, however, the pellets did not present good cohesion, being necessary the use of a binder. The authors tested three types of binders in three different proportions, and the best results were obtained with 30% w w^{-1} of cellulose. In some cases, materials used as binders (e.g. cellulose) may have another purpose. In this sense, Augusto et al. [28] proposed a preparation of milk powder samples using microcrystalline cellulose as analytical blank. In addition, cellulose-milk mixtures were prepared in different proportions. These mixtures were pressed into pellets and analyzed directly by LIBS. Another strategy for the preparation of solid samples is the use of an adhesive tape, where a small amount of powdered sample is retained. This strategy is recommended when the amount of sample is not enough to prepare a pellet. Using this procedure, Silva et al. [29] developed

a rapid method for identifying gunshot residues composed of Pb from the initiator, Ba from the oxidant and Sb from the fuel. Several volunteers were selected to carry out shots and after this process, the authors collected the material with adhesive tape from the volunteer's hand. Adhesive tapes containing the particles from the shots were taken directly for analysis in LIBS. From the characteristic elements of gunpowder, classification models were proposed using the soft independent modeling of class analogies (SIMCA), for the identification of shooter.

For the preparation of liquid samples, some additional problems may arise [30]. The laser-matter interaction is affected since part of the laser energy is dissipated by spreading the sample (splashing). As a consequence, the reproducibility and repeatability of the analyses are drastically deteriorated. In addition, the plasma temperature is compromised (lower temperature), making the excitation/atomization of the species present in the sample more difficult. In order to circumvent these undesirable effects, some preparation strategies have been proposed and generally involve the matrix conversion of the liquid into a solid. The most common strategy is simply freezing aqueous samples and subsequent analysis of the resulting solid [31]. In a study proposed by Lee et al. [32], the authors used a peristaltic pump to produce a sample jet in which the laser pulse was directly irradiated. Other strategies involve the transfer of the liquid sample to non-permeable substrates such as graphite [33] and metal plate [34], or to permeable substrates such as filter paper [35]. In these cases, the liquid sample is deposited on these substrates and, after drying the material, the substrate is analyzed. In this way, the problems inherent in liquid analysis are minimized, and the analysis process occurs in a manner analogous to solid samples.

1.4. Chemometrics

The term "chemometrics" was firstly introduced by Svante Wold in 1971. Chemometrics is related to the use of mathematical models and statistical principles on analytical chemistry datasets. Chemometrics is nowadays a science that is becoming popular among modern researchers due to its capability of extract the most important information along huge datasets produced in analytical instruments (e.g. LIBS) and it is currently defined as multidisciplinary approach that includes mathematics and statistics [36,37]. Technological advances improved the development of several computational and statistical algorithms to accomplish this task. Nowadays the variety of chemometric tools existing is high and the selection of them will depend on the desired analytical application [38]. As mentioned before, LIBS analysis generates huge datasets (normally more than ten thousand variables), being the use of chemometrics indispensable in almost all cases, mainly those intended to classification and multivariate calibration. Several factors, such as fluctuations in laser pulse energy, ablation rate, and laser-matter interaction make LIBS analysis complex, thus, improvements in the accuracy of qualitative and quantitative analyses are required, minimizing drawbacks in obtaining and interpreting maximum useful data information. Hence, the success of combining LIBS with the use of chemometric tools, which help to better understand the spectral data, is well known [36]. It is recommended that the datasets be preprocessed before applying any chemometric tool to the LIBS data, due to the complexity of laser-sample and laser-plasma interactions and the sensitivity of plasma to the physical and chemical characteristics of the samples. In this way, data normalization or standardization is of great importance as it minimizes unwanted variations avoiding problems in future analyses. There are several types of

normalizations that can be employed for this purpose, such as: normalization by the total spectrum area, by the signal that presents higher intensity, using the Euclidean norm, internal standardization [22], among others. There are other types of preprocesses employed in LIBS data, such as meancentering (all spectra subtracted by the average spectrum) for cases where the full spectral profile is used and auto-scaling (division of the spectra meancentered by the standard deviation value) for situations where the area or height of several selected regions are employed (normally after a variable selection). Both are widely used in exploratory data analysis, classification and calibration models proposition [39,40].

Chemometrics can be divided into four main blocks: (i) design of experiments (DoE) and surface response methodology (SRM); (ii) exploratory analysis of chemical data; (iii) classification models; and (iv) multivariate calibration [41,45]. In LIBS analysis, it is essential to optimize the instrumental parameters such as: laser pulse fluence (parameter that relates laser pulse energy and spot size) and delay time which are commonly optimized through experimental design to obtain an optimal or compromise condition [46-50]. Supervised pattern recognition methods using SIMCA, partial least squares discriminant analysis (PLS DA), k-nearest neighbor (KNN), and linear discriminant analysis (LDA) chemometric tools are widely used in LIBS [36] when the goal is to use spectral information for proposing classification models. These tools have been successfully employed in proposing classification models for a wide variety of samples [22,23,51-58]. Another widely used chemometric approach in LIBS analysis is the multivariate calibration. Inside this block, partial least squares (PLS) [59], multiple linear regression (MLR) [60], artificial neural networks (ANN) [61] arise as some of the main multivariate calibration tools used, among others [36,62,63]. As it can be noted, the

application of chemometrics to LIBS spectral data is wide. Despite extracting and maximizing useful information and improving the accuracy of qualitative and quantitative analyses, the chemometric universe applied to LIBS still requires further exploration and research to improve the technique's performance in several fields of application.

1.5. Goals

The overall goal of this thesis was the development of sample preparation procedures for difficult-to-mineralize materials, focusing direct analysis by laser-induced breakdown spectroscopy (LIBS).

The specific goals were:

- Determination of Al, Cr, Fe, Mg, Mn, and Ni on nickeliferous mineral ores through a different sample preparation of powdered samples for LIBS analysis.

- Evaluating the possibilities of LIBS for direct analysis of solder mask samples intended for homemade production of PCB, focusing the determination of Ba content on these materials.

- Assessment of uni and multivariate calibration tools for determination of Ti content on sunscreen.

1.6. References

[1] ABAD-PEÑA, E.; LARREA-MARÍN, M. T.; VILLANUEVA-TAGLE, M. E.; POMARES-ALFONSO, M. S. "Multielemental inductively coupled plasma optical emission spectrometry analysis of nickeliferous minerals". Talanta. 124: 79 – 88, 2014

[2] SPERANÇA, M. A.; POMARES-ALFONSO, M. S.; PEREIRA-FILHO, E. R. "Analysis of Cuban nickeliferous minerals by laser-induced breakdown spectroscopy (LIBS): non-conventional sample preparation of powder samples". Anal. Methods. 10: 533 – 540, 2018.

[3] COTO, O.; GALIZIA, F.; HERNÁNDEZ, I.; MARRERO, J.; DONATI, E. Cobalt and nickel recoveries from laterite tailings by organic and inorganic bio-acids". Hydrometallurgy. 94: 18 – 22, 2008

[4] BROEKAERT, J. A. C. "State-of-the-art and trends of development in analytical atomic spectrometry with inductively coupled plasmas as radiation and ion sources". Spectrochim. Acta, Part B. 55: 739 – 751, 2000.

[5] C. Yang, Z.-G. Yang. Synthesis of Low Viscosity, Fast UV Curing Solder Resist Based on Epoxy Resin for Ink-Jet Printing''. J. Appl. Polym. Sci. 2013. 129(1): 187–192.

[6] HOFMEISTER, C.; MAASS, S.; FLADUNG, T.; MAYER, B. "evaluation of process influences on surface chemistry of epoxy acrylate based solder mask via XPS, ToF-SIMS and contact angle measurement''. Mater. Chem. Phys. 185: 129–136, 2017.

[7] WENK, K. S.; EHRLICH, A. "Allergic contact dermatitis from epoxy resin in solder mask coating in an individual working with printed circuit boards''. Dermatitis. 21(5): 288 – 291, 2010

[8] SPERANÇA, M. A.; VIRGILIO, A.; PEREIRA-FILHO, E. R.; AQUINO, F. W. B. "Determination of elemental content in solder mask samples used in printed circuit boards using different spectroanalytical techniques". Appl. Spectrosc. 72(8): 1205 – 1214, 2018.

[9] ROHLOFF, R.R. Solder mask composition. US4252888A. Filed 1980. Issued 1981.

[10] SERENSON Jr, J.A.; MARONGELLI, S. "The effect of solder mask and surface mount adhesive types on a PCB manufacturing process". Proceedings of the Technical Program (West and East), National Electronic Packaging and Production Conference. 2: 731–746, 1999.

[11] SERPONE, N.; DONDI, D.; ALBINI, A. "Inorganic and organic UV filters: their role and efficacy in sunscreens and suncare products". Inorg. Chim. Acta. 360: 794 – 802, 2007.

[12] SPERANÇA, M. A.; ANDRADE, D. F.; CASTRO, J. P.; PEREIRA-FILHO, E. R. "Univariate and multivariate calibration strategies in combination with laser-induced breakdown spectroscopy (LIBS) to determine Ti on sunscreen: a different sample preparation procedure". Opt. Laser Technol. 360: 794 – 802, 2019.

[13] FORTES, F. J.; MOROS, J.; LUCENA, P.; CABALÍN, L. M.; LASERNA, J. J. "Laser-induced breakdown spectroscopy". Anal. Chem. 85: 640 – 669, 2013.

[14] HAHN, D. W.; OMENETTO, N. "Laser-induced breakdown spectroscopy (LIBS), part I: review of basic diagnostics and plasma-particle interactions: still-challenging issues within the analytical plasma community". Appl. Spectrosc. 64(12): 335A – 366A, 2010.

[15] HAHN, D. W.; OMENETTO, N. "Laser-induced breakdown spectroscopy (LIBS), part II: review of instrumental and methodological approaches to material analysis and applications to different fields". Appl. Spectrosc. 66(4): 347 – 419, 2012.

[16] PASQUINI, C.; CORTEZ, J.; SILVA, L. M. C.; GONZAGA, F. B. "Laser-induced breakdown spectroscopy". J. Braz. Chem. Soc. 18(3): 463 – 512, 2007.

[17] COSTA, V. C.; AUGUSTO, A. S.; CASTRO, J. P.; MACHADO, R. C.; ANDRADE, D. F.; BABOS, D. V.; SPERANÇA, M. A.; GAMELA, R. R.; PEREIRA-FILHO, E. R. "Laser induced-breakdown spectroscopy (LIBS): histórico, fundamentos, aplicações e potencialidades". Quim. Nova. 42(5): 527 – 545, 2019.

[18] JANTZI, S. C.; MOTTO-ROS, V.; TRICHARD, F.; MARKUSHIN, Y.; MELIKECHI, N.; DE GIACOMO, A. "Sample treatment and preparation for laser-induced breakdown spectroscopy" Spectrochim. Acta, Part B, 115: 52 – 63, 2016.

[19] KRUG, F. J.; ROCHA, F. R. P. Métodos de preparo de amostras. Fundamentos sobre o preparo de amostras orgânicas e inorgânicas para análise elementar, EditSBQ: São Paulo, 2016.

[20] JULL, H.; KUNNEMEYER, R.; SCHAARE, P. "Nutrient quantification in fresh and dried mixtures of ryegrass and clover leaves using laser-induced breakdown spectroscopy". Precision Agric. 19, 823 – 839, 2018.

[21] CAHOON, E. M.; ALMIRALL, J. R. "Wavelength dependence on the forensic analysis of glass by nanosecond 266 nm and 1064 nm laser induced breakdown spectroscopy". Appl. Opt. 49: 49 – 57, 2010.

[22]. CASTRO, J. P; PEREIRA-FILHO, E. R. "Twelve different types of data normalization for the proposition of classification, univariate and multivariate regression models for the direct analyses of alloys by laser-induced breakdown spectroscopy (LIBS)". J. Anal. At. Spectrom. 31: 2005 – 2014, 2016.

[23] COSTA, V. C.; AQUINO, F. W. B.; PARANHOS, C. M.; PEREIRA-FILHO, E. R. "Identification and classification of polymer e-waste using laser-induced breakdown spectroscopy (LIBS) and chemometric tools". Polym. Test. 59: 390 – 395, 2017.

[24] SPERANÇA, M. A.; AQUINO, F. W. B.; FERNANDES, M. A.; LOPEZ-CASTILLO, A.; CARNEIRO, R. L.; PEREIRA-FILHO, E. R. "Application of laser-induced breakdown spectroscopy and hyperspectral images for direct evaluation of chemical elemental profiles of coprolites". Geostand. Geoanal. Res., 41(2): 273 – 282, 2016.

[25] FIGUEIREDO, C. M.; CASTRO, J. P.; SPERANÇA, M. A.; FIALHO, L. L.; NÓBREGA, J. A.; PEREIRA-FILHO, E. R. "Qualitative and quantitative chemical investigation of orthopedic alloys by combining wet digestion, spectroanalytical methods and direct solid analysis". J. Braz. Chem. Soc., 29(4): 680 – 688, 2018.

[26] BABOS, D. V.; VIRGILIO, A.; COSTA, V. C.; DONATI, G. L.; PEREIRA-FILHO, E. R. "Multi-energy calibration (MEC) applied to laser-induced breakdown spectroscopy (LIBS)". J. Anal. At. Spectrom. 33: 1753 – 1762, 2018.

[27] PERUCHI, L. C.; NUNES, L. C.; CARVALHO, G. G. A.; GUERRA, M. B. B.; ALMEIDA, E.; RUFINI, I. A.; SANTOS, D.; KRUG, F. J. "Determination of inorganic nutrients in wheat flour by laser-induced breakdown spectroscopy and energy dispersive X-ray fluorescence spectrometry". Spectrochim. Acta, Part B, 100: 129 – 136, 2014

[28]. AUGUSTO, A. S.; BARSANELLI, P. L.; PEREIRA, F. M. V.; PEREIRA-FILHO, E. R. "Calibration strategies for the direct determination of Ca, K, and Mg in commercial samples of powdered milk and solid dietary supplements using laser-induced breakdown spectroscopy (LIBS)". Food Res. Int., 94: 72 – 78,2017.

[29] SILVA, M. J.; CORTEZ, J.; PASQUINI, C.; HONORATO, R. S.; PAIM, A. P. S.; PIMENTEL, M. F. "Gunshot residues: screening analysis by laser-induced breakdown spectroscopy". J. Braz. Chem. Soc., 20(10): 1887 – 1894, 2009.

[30] HARUN, H. A.; ZAINAL, R. "Laser-induced breakdown spectroscopy measurement for liquids: experimental configurations and sample preparations". J. Nonlinear Opt. Phys. Mater. 27(2): 1850023 – 1850054, 2018.

[31] SOBRAL, H.; SANGINÉS, R.; TRUJILLO-VÁZQUEZ, A. "Detection of trace elements in ice and water by laser-induced breakdown spectroscopy". Spectrochim. Acta, Part B., 78: 62 – 66, 2012.

[32] LEE, D. H.; HAN, S. C.; KIM, T. H.; YUN, J. I. "Highly sensitive analysis of boron and lithium in aqueous solution using dual-pulse laser-induced breakdown spectroscopy". Anal. Chem. 83: 9456 – 9461, 2011.

[33] SARKAR, A.; AGGARWAL, S. K.; ALAMELU, D. "Laser induced breakdown spectroscopy for rapid identification of different types of paper for forensic application". Anal. Methods. 2: 32 – 36, 2010.

[34] YANG, X.; HAO, Z.; LI, C.; LI, J.; YI, R.; SHEN, M.; LI, K.; GUO, L.; LI, X.; LU, Y. "Sensitive determinations of Cu, Pb, Cd, and Cr elements in aqueous solutions using chemical replacement combined with surface-enhanced laser-induced breakdown spectroscopy". Opt. Express. 24: 13410 – 13417, 2016.

[35] YAROSHCHYK, P.; MORRISON, R. J.; BODY, D.; CHADWICK, B. L. "Quantitative determination of wear metals in engine oils using laser-induced breakdown spectroscopy: a comparison between liquid jets and static liquids". Spectrochim. Acta, Part B. 60: 986 – 992, 2005.

[36] ZHANG, T.; TANG, H.; Li, H. "Chemometrics in laser-induced breakdown spectroscopy". J. Chemom., 11: 2983 – 3000, 2018.

[37] NOVAES, C. G.; YAMAKI, R. T.; DE PAULA, V. F.; JÚNIOR, B. B. N.; BARRETO, J. A.; VALASQUES, G. S.; BEZERRA, M. A. "Otimização de métodos analíticos usando metodologia de superfícies de resposta - parte I: variáveis de processo". Rev. Virtual Quim., 9:1184 – 1215, 2017.

[38] MONCAYO, S.; MANZOOR, S.; NAVARRO-VILLOSLADA, F.; CACERES, J. O. "Evaluation of supervised chemometric methods for sample classification by laser-induced breakdown spectroscopy". Chemom. Intell. Lab. Syst., 146:354 – 364, 2015.

[39] BRO, R.; SMILDE, A. K. "Principal component analysis". Anal. Methods., 6:2812 – 2831, 2014.

[40] PORIZKA, P.; KLUS, J.; KÉPES, E.; PROCHAZKA, D.; HAHN, D. W.; KAISER, J. "On the utilization of principal component analysis in laser-induced breakdown spectroscopy data analysis, a review". Spectrochim. Acta, Part B, 148:65 – 82, 2018.

[41] BEZERRA, M. A.; FERREIRA, S. L. C.; NOVAES, C. G.; SANTOS, A. M. P.; VALASQUES, G. S.; CERQUEIRA, U. M. F. M.; ALVES, J. P. S. "Simultaneous optimization of multiple responses and its application in analytical chemistry–a review". Talanta, 194:941 – 959, 2019.

[42] PEREIRA, F. M. V.; PEREIRA-FILHO, E. R. "Application of free computational program in experimental design: a tutorial". Quim. Nova, 41:1061 – 1071, 2018.

[43] NOVAES, C. G.; YAMAKI, R. T.; NASCIMENTO, JR. B. B.; BARRETO, J. A.; VALASQUES, G. S.; BEZERRA, M. A. "Otimização de métodos analíticos usando metodologia de superfícies de respostas - parte II: variáveis de mistura". Rev. Virtual Quim., 10:393 – 420, 2018.

[44] PASSARI, L. M. Z. G.; SOARES, P. K.; BRUNS, R. R. "Estatística aplicada à química: dez dúvidas comuns". Quim. Nova, 34:888 – 892, 2011.

[45] PIMENTEL, M. F.; BARROS-NETO, B. "Calibração: uma revisão para químicos analíticos". Quim. Nova, 19:268 – 277, 1996.

[46] FORTUNATO, F. M.; CATELANI, T. A.; ALFONSO, M. S. P.; PEREIRA-FILHO, E. R. "Application of multi-energy calibration for determination of chromium and nickel in nickeliferous ores by laser-induced breakdown spectroscopy". Anal. Sci. 35:165 – 168, 2018.

[47] ANDRADE, D. F.; PEREIRA-FILHO, E. R.; KONIECZYNSKI, P. "comparison of ICP OES and LIBS analysis of medicinal herbs rich in flavonoids from Eastern Europe". J. Braz. Chem. Soc., 28:838 – 847, 2017.

[48] NUNES, L. C.; DA SILVA, G. A.; TREVIZAN, L. C.; SANTOS JR, D.; POPPI, R. J.; KRUG, J. F. "Simultaneous optimization by neuro-genetic approach for analysis of plant materials by laser induced breakdown spectroscopy". Spectrochim. Acta, Part B, 64:565 – 572, 2009.

[49] NUNES, L. C.; BRAGA, J. W. B.; TREVIZAN, L. C.; SOUZA, P. F.; CARVALHO, G. G. A.; SANTOS JR, D.; POPPI, R. J.; KRUG, F. J. "Optimization and validation of a LIBS method for the determination of macro and micronutrients in sugar cane leaves". J. Anal. At. Spectrom., 25:1453 – 1460, 2010.

[50] FERREIRA, E. C.; ANZANO, J. M.; MILORI, D. M. B. P.; FERREIRA, E. J.; LASHERAS, R. J.; BONILLA, B.; MONTULLIBOR, B.; CASAS, J.; MARTIN-NETO, L. "Multiple response optimization of laser-induced breakdown spectroscopy parameters for multi-element analysis of soil samples". Appl. Spectrosc., 63:1081 – 1088, 2009.

[51] NEIVA, A. M.; CHAGAS, M. A. J.; MELLO, M. A.; ESTEVES, S. N.; PEREIRA-FILHO, E. R. "Proposition of classification models for the direct evaluation of the quality of cattle and sheep leathers using laser-induced breakdown spectroscopy (LIBS) analysis". RSC Adv., 6:104827 – 104838, 2016.

[52] AUGUSTO, A. S.; BATISTA, E. F.; PEREIRA-FILHO, E. R. "Direct chemical inspection of eye shadow and lipstick solid samples using laser-induced breakdown spectroscopy (LIBS) and chemometrics: proposition of classification models". Anal. Methods, 8:5851 – 5860, 2016.

[53] BORBA, F. S. L.; CORTEZ, J.; ASFORA, V. K.; PASQUINI, C.; PIMENTEL, M. F.; PESSISE, A. M.; KHOURY, H. J. "Multivariate treatment of libs data of prehistoric paintings". J. Braz. Chem. Soc., 23:958 – 965, 2012.

[54] YANG, J. H.; YOH, J. J. "Forensic discrimination of latent fingerprints using laser-induced breakdown spectroscopy (LIBS) and chemometric approaches". Appl. Spectrosc., 72:1047 – 1056, 2018.

[55]. HARMON, R. S.; RUSSO, R. E.; HARK, R. R. "Applications of laser-induced breakdown spectroscopy for geochemical and environmental analysis: a comprehensive review". Spectrochim. Acta, Part B, 87:11 – 26, 2013.

[56] GUEDES, W. N.; PEREIRA, F. M. V. "Classifying impurity ranges in raw sugarcane using laser-induced breakdown spectroscopy (LIBS) and sum fusion across a tuning parameter window". Microchem. J., 143:331 – 336, 2018.

[57] CHEN, X.; LI, X.; YU, X.; CHEN, D.; LIU, A. "Diagnosis of human malignancies using laser-induced breakdown spectroscopy in combination with chemometric methods". Spectrochim. Acta, Part B, 139:63 – 69, 2018.

[58] LI, X.; YANG, S.; FAN, R.; YU, X.; CHEN, D. "Discrimination of soft tissues using laser-induced breakdown spectroscopy in combination with k nearest neighbors (kNN) and support vector machine (SVM) classifiers". Opt. Laser Technol., 102:233 – 239, 2018.

[59] GOMÉZ-NUBLA, L.; ARAMENDIA, J.; DE VALLEJUELO, S. F-O.; MADARIAGA, J. M. "Analytical methodology to elemental quantification of weathered terrestrial analogues to meteorites using a portable laser-induced breakdown spectroscopy (LIBS) instrument and partial least squares (PLS) as multivariate calibration technique". Microchem. J., 137:392 – 401, 2018.

[60] SPERANÇA, M. A.; ANDRADE, D. F.; CASTRO, J. P.; PEREIRA-FILHO, E. R. "Univariate and multivariate calibration strategies in combination with laser-induced breakdown spectroscopy (LIBS) to determine Ti on sunscreen: a different sample preparation procedure". Opt Laser Technol., 109:648 – 653, 2019.

[61] SAFI, A.; CAMPANELLA, B.; GRIFONI, E.; LEGNAIOLI, S.; LORENZETTI, G.; PAGNOTTA, S.; POGGIALINI, F.; RIPOLL-SEGUER, L.; HIDALGO, M.; PALLESCHI, V. "Multivariate calibration in laser-induced breakdown spectroscopy quantitative analysis: the dangers of a 'black box' approach and how to avoid them". Spectrochim. Acta, Part B, 144:46 – 54, 2018.

[62] ROMERA, J. P. R.; BARSANELLI, P. L.; PEREIRA, F. M. V. "Expeditious prediction of fiber content in sugar cane: an analytical possibility with LIBS and chemometrics". Fuel, 166:473 - 476, 2016.

[63] BRAGA, J. W. B.; TREVIZAN, L. C.; NUNES, L. C.; RUFINI, I. A.; SANTOS JR, D.; KRUG, F. J. "Comparison of univariate and multivariate calibration for the determination of micronutrients in pellets of plant materials by laser induced breakdown spectrometry". Spectrochim. Acta, Part B, 65:66 – 74, 2010

Chapter 2 – Nickeliferous minerals

2.1. Chapter Outline

Cuba presents the largest deposits of minerals containing nickel, with approximately 40 % of the worldwide natural reserves. This means that the mining of this element represents great importance for the Cuban economy. The monitoring of these materials is a complicated step on the quality control of them, requiring the use of strong acid mixtures followed by microwave assisted mineralization or furnaces with high temperatures. Despite of being reliable and routinely implemented, ICP OES analysis needs these laborious, time-consuming, and several preparation steps to be performed. On the other hand, with the high concentrations monitored on the samples, LIBS appears to be a good alternative on this analytical problem. The most used sample preparation for powdered samples for LIBS consists on pressing the material into pellets, but this procedure presents some problems of microheterogeneity, and high roughness of the pellet when the samples have high content of Si. In this context, the goal of this study was to propose a different sample preparation for powdered mineral samples diluting them with water and then immobilizing the material with a PVA aqueous solution 10 % w v^{-1} for further LIBS analysis. This strategy enables the possibility of adding internal standard elements for further normalization procedures to minimize some problems, such low reproducibility due to effects on laser-matter interaction, and severe matrix interferences. The creation of univariate calibration models for Al, Cr, Fe, Mg, Mn, and Ni were calculated for a set of 33 samples and 2 certified reference materials of nickeliferous minerals. The reference results were obtained on routine laboratories in Cuba with ICP OES analysis and the concentration range were for Al: 0.49 to 26.82 %, for Cr: 0.40 to 2.21 %, for Fe: 6.8 to 52.93 %, for Mg: 0.41 to 20.53 %, for Mn: 0.11 to 1.50 %, and for Ni: 0.23 to 3.02 %. The standard error of validation (SEV) were 1.34, 0.16, 6.08, 0.88, 0.09, and 0.35 % for

Al, Cr, Fe, Mg, Mn, and Ni, respectively. The good results make this strategy a reliable alternative for faster and safer sample preparation for LIBS analysis. The internal standard addition was effective but the results were not improved over the already tested normalization procedures.

2.2. Analysis of Cuban nickeliferous minerals by laser-induced breakdown spectroscopy (LIBS): nonconventional sample preparation of powder samples

FIGURE 2.1 – Sample preparation for Cuban nickeliferous minerals for direct LIBS analysis.

Check for updates

Analysis of Cuban nickeliferous minerals by laser-induced breakdown spectroscopy (LIBS): non-conventional sample preparation of powder samples

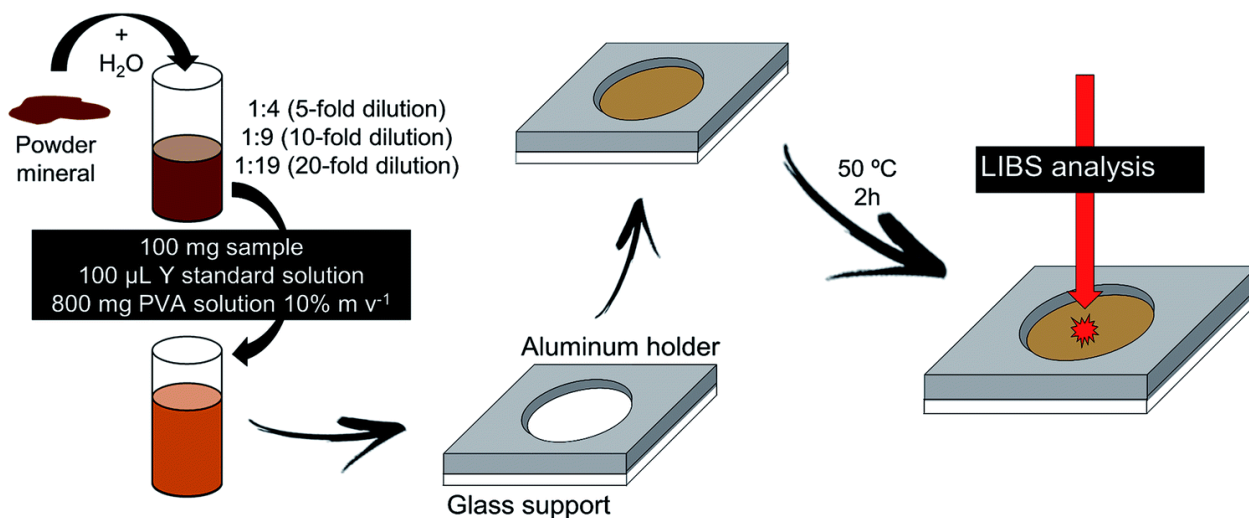Marco Aurelio Sperança, [ID] [a] Mario Siméon Pomares-Alfonso[b] and Edenir Rodrigues Pereira-Filho [ID] *[a]

In the present study, a new method to quantify Al, Cr, Fe, Mg, Mn, and Ni in nickeliferous minerals by laser-induced breakdown spectroscopy (LIBS) is proposed. Thirty-three mineral powder solid samples, previously analyzed by inductively coupled plasma optical emission spectroscopy (ICP OES), and two certified reference materials were used as reference samples for the calibration, and an innovative sample preparation was implemented and described. The use of Bi, Sc and Y as internal standards and the usefulness of other normalization modes were assessed in the normalization of the LIBS emission signals from the analytes. A slurry was made by mixing the solid mineral samples, grinding them into a fine powder, and using water in different proportions. Then, the mixture was homogenized and instantly weighed with a constant mass of a standard liquid solution of Y, which was preliminarily chosen as the internal standard among the three elements assessed, and a 10% (w v^{-1})-polyvinyl-alcohol solution. After 2 h in an oven at 50 °C, the samples, which were immobilized in the polymer film, were subjected to LIBS analysis. The best sample dilution, emission line and normalization of the emission signal were selected for each analyte. The concentrations of the assessed analytes varied from 0.49 to 26.82% for Al, 0.40 to 2.21% for Cr, 6.8 to 52.93% for Fe, 0.41 to 20.53% for Mg, 0.11 to 1.50% for Mn and 0.23 to 3.02% for Ni. The standard error of validation (SEV) for the newly developed method was 1.34, 0.16, 6.08, 0.88, 0.09, and 0.35% for Al, Cr, Fe, Mg, Mn, and Ni, respectively.

Introduction

The sample preparation step presents several challenges in any analytical technique. In most cases, homogeneous liquid samples must be prepared to be introduced into instruments. Laser-induced breakdown spectroscopy (LIBS), despite the direct use of solid samples, has several limitations in the calibration of both solid and liquid sample analyses. In the literature, several papers have presented alternatives for solid sample analyses,[1,2] and some reviews are available describing strategies for liquid sample analyses.[3–5]

The preparation of solid samples usually consists of pelletizing the sample into a rough pellet that is intended to be homogeneous with respect to the concentrations of all the elements of interest and representative of the whole sample type considered. In this case, it is really important that the samples are in the form of a fine powder, which requires a milling process.[4] Regarding mineral samples, this process can be difficult because these types of samples are generally rough. Another severe drawback faced in this strategy is the mill used, as the milling tools (knife and balls) must not be composed of the elements that will be later assessed in the minerals, *e.g.*, iron, copper, and nickel. The homogeneity is another point that should be addressed because it is not always possible to guarantee homogeneity in such materials. One common strategy employed to minimize this problem is to use an average spectrum from a high number of LIBS pulses obtained from the surface of the pellets.[6]

As far as liquid samples are concerned, the LIBS analysis can be extremely difficult, and there are several inherent problems reported in the literature, such as splashing, surface ripples, heterogeneity of the plasma on the liquid surface, shorter plasma duration, and poor reproducibility and repeatability.[3,5] To overcome these problems, there are two main classes of strategies employed. One consists of finding a more appropriate experimental configuration, and the second is generally a conversion of the liquid sample to a solid one. The use of laminar flows and jets[7] in regard to the sample presentation and the use of the double-pulse mode[8] in regard to the instrumental

[a]Department of Chemistry, Federal University of São Carlos, São Carlos, São Paulo State, 13565-905, Brazil. E-mail: erpf@ufscar.br; Fax: +55 16 3351 8350; Tel: +55 16 3351 8092

[b]Institute of Materials Science and Technology (IMRE), University of Havana, Havana, 10400, Cuba

25

setup, illustrate the first strategy. The majority of studies have used the second strategy, and freezing,[9,10] adsorption on a substrate and conversion to a liquid-to-solid matrix are some of the examples of the second strategy.[11] In the study of Andrade *et al.* (2017)[12] the authors described a similar methodology to the one that will be shown in this study, for LIBS analysis of liquid mineral fertilizers. The results were appreciable and highlighted the efficiency of the liquid-to-matrix conversion process with a minimal sample preparation.

Mineral samples are known to be materials that are difficult to decompose by wet digestion. Several stages are necessary for their total solubilization, and these steps are often dangerous and laborious and can introduce errors in the measurements.[13] Cuba has been among the countries with the largest deposits of minerals containing nickel (nickeliferous minerals), approximately 40% of the natural reserves of nickel,[14] and the nickel industry represents one of the most important sectors of the economy in that country.[15] Currently nickeliferous minerals are digested by melting them with some mixed fluxes[14,16,17] and then dissolving them with hydrochloric or nitric acid. Alternative methods may be employed, such as microwave assisted acid digestion, using acid mixtures such as aqua-regia ($HCl : HNO_3$ = 3 : 1) followed by the addition of hydrofluoric or nitric acid with perchloric acid and, finally, the addition of hydrofluoric acid to completely leach the metals strongly bound in the crystalline structure.[14,18–20] Simultaneously, the sample digestion with dangerous reagents generates residues that are harmful to the environment, which is particularly of significant concern in routine laboratories, where thousands of these samples are annually analyzed. In contrast, the LIBS analysis does not require the digestion of solid samples, avoiding the drawbacks previously mentioned. On the other hand, the limit of detection of LIBS determination achieved by using the commercially available LIBS spectrometers is generally worse than those achieved by ICP OES. Unquestionably, this is one of the main challenges to be overcome in LIBS analysis. However, and keeping in mind this inconvenience, the implementation of a LIBS method for the determination of main constituents in nickeliferous minerals could be an invaluable tool for the routine analysis in geological services laboratories around the world.

In this context, the goal of this study was to develop a different solid sample preparation for LIBS analysis to reduce the fluctuations in the signals, improve the homogeneity of samples and to propose a simpler, faster and safer method than the traditional one to determine Al, Cr, Fe, Mg, Mn, and Ni contents in nickeliferous minerals. The incorporation of internal standard elements (Bi, Sc and Y) as solutions into the solid samples and the usefulness of normalization modes were assessed along with the proposed sample preparation.

Experimental

Instrumental LIBS setup

For all LIBS measurements, a J200 commercial system from Applied Spectra (Freemont, CA, USA) was used. This system is equipped with a Nd:YAG 1064 nm laser, a CCD (charge-coupled device) spectrometer that sweeps 12 288 emission lines from 186 to 1042 nm, and an automated XYZ stage with a 1280 × 1024 CMOS (complementary metal-oxide semiconductor) color camera imaging system. Additionally, software manages the operational parameters, which include the laser pulse energy, delay time, spot size, laser frequency and speed of the ablation chamber during raster experiments. The laser pulse energy, delay time and spot size were thoroughly assessed by using the Doehlert design with a laser pulse energy of 30 to 80 mJ, a delay time of 0 to 2 μs, and a spot size of 50 to 150 μm, whereas the laser frequency, raster speed and gate width were fixed at 5 Hz, 1 mm s^{-1}, and 1.05 ms, respectively.

Reagents, standards and samples

Polyvinyl alcohol (PVA) from Matheson Coleman & Bell (Ohio, USA) was used for sample preparation. A 10% (w v^{-1}) PVA solution was prepared with deionized water (resistivity > 18.2 MΩ cm) produced using a Milli-Q® Plus Total Water System (Millipore Corp., Bedford, MA, USA). A Y standard of 1.000 mg g^{-1} (0.999 mg g^{-1} ± 0.003 mg g^{-1}) was used as an internal standard. Thirty-three samples of Cuban nickeliferous minerals provided by Ana Teresa Acebal Ibarra from Elio Trincado Laboratory, Geominera Oriente Enterprise – Santiago de Cuba, Cuba and 2 certified reference materials "Nickeliferous Laterite (L-1)" and "Nickeliferous Serpentinite (SNi)" manufactured by the Central Laboratory of Minerals José Isaac del Corral (LACEMI) were used throughout the experiments. The concentrations of the major elements in the thirty-three samples represent the whole concentration range of the elements to be determined in the present study, while both types of minerals considered for the preparation of L-1 and SNi are the most important since they represent 60% of the Cuban nickeliferous minerals that are of economic interest.

The concentrations of Al, Cr, Fe, Mg, Mn and Ni in the thirty-three reference mineral samples were determined according to the appropriate guidelines developed in Cuban laboratories.[14] In brief, the sample test portion was digested by using a fusion technique with lithium metaborate (sample : lithium metaborate = 1 : 7.5). Then, the sample was dissolved in hydrochloric acid. The sample dissolutions were analyzed using an ICP OES Spectroflame or ICP OES Spectro Arcos (Spectro Analytical Instruments, Germany) under routine operating conditions, which were previously validated.

Sample preparation for LIBS determination

The proposed sample preparation involved an encapsulation/immobilization of the powder solid samples with PVA solution. The mineral solid powder samples were first dispersed in deionized water to form suspensions in different sample/water proportions (1 : 4, 1 : 9, 1 : 19). For this, 0.2000 g was accurately weighed, and the corresponding water mass was also weighed (0.8000, 1.8000 and 3.8000 g) in a 15 ml falcon tube. The PVA solution was prepared by weighing the corresponding mass to form a 10% (w v^{-1}) solution and dissolving it in hot water (150 °C) with constant stirring.

In a 2 ml tube, 0.1000 g of the sample suspension was weighed and stirred to guarantee homogeneity. After that, 0.1000 g of the Y standard, 1.000 mg g^{-1}, was weighed, and 0.8000 g of the 10% (w v^{-1}) PVA solution was added into the tube. The mixture was homogenized with a vortex mixer. This mixture was then placed in a support specifically designed for this experiment, which consisted of an aluminum holder held by clips on a glass support. This process is depicted in Fig. 1. The support with the sample was placed in an oven for 2 h at 50 °C. Three authentic replicate samples ($n = 3$) for each of the three suspensions were prepared, and in each replicate, approximately 500 LIBS pulses were performed.

LIBS data treatment

All LIBS data for the samples obtained from the instrument were first treated with a homemade MATLAB® version 2017b, which is a variation of the script thoroughly explained by Castro & Pereira-Filho.[21] This first script returns a matrix with 12 columns. Each column corresponds to one type of the twelve normalizations assessed in this study. The first column just returns the analyte signals averaged for all the spectra collected in a sample. After normalization, the normalized analyte signal was averaged for all the spectra collected from the sample. Therefore, the twelve columns returned by the script were: (1) the average analyte signal for all the collected spectra, (2) the average of the analyte signal normalized by the norm, (3) the average of the analyte signal normalized by the height of the highest analyte signal in the spectrum, (4–5) the average of the analyte signal normalized by the intensities of the lines 193.090 nm and 247.860 nm for carbon, (6–11) the average of the analyte signal normalized by the intensity of the lines 371.030 nm, 360.070 nm, 377.430 nm, 488.370 nm, 324.228 nm and 437.490 nm for Y, and (12) the average of the analyte signal normalized by the sum of 12 288 signals, meaning, all the emission signals were registered in a spectrum. The addition of several Y lines in this script was made after a preliminary assessment of Bi, Sc, and Y as internal standards, and the lines used for the normalization of the analyte signal were 472.252 nm, 508.156 nm and 371.030 nm, respectively. Fig. 2

shows a pictorial description of the normalization process applied in this study: hypothetical spectra ($n = 3$) containing C, Y and analyte (green) emission lines are presented. After normalization by C and Y emission lines the corresponding line signal height (red) is equal to one.

In this first described script, the analyte signals used were not background corrected. Then, another homemade script selected the spectral region around the emission line of interest, and a baseline correction (subtraction) was done. After that, the second script calculates: (a) the signal-to-background ratio (SBR) using the analyte signal with the highest background-corrected intensity and the average of the nearest background of that signal and (b) the sum of all the signals under the peak, *i.e.*, the area in the selected spectral region close to the emission line of the highest intensity signal. Once the SBR and the area under the peak were calculated, a matrix was created with these two parameters in each column and 12 rows, representing the average of the analyte signal without normalization of all the collected spectra and each of the normalizations assessed (previously described, see also Fig. 2). Furthermore, an Excel® template was prepared to calculate univariate calibration models using as independent variable "*y*" the area under the peak of the normalization signals described previously in the first script. The standard error of calibration (SEC) for each analyte was calculated as follows:

$$SEC = \sqrt{\sum_{i=1}^{n} \frac{(y_i - \hat{y}_i)^2}{n-1}}$$

where n is the number of samples used in the calibration model, y_i is the reference concentration obtained previously by ICP OES, and $\hat{y}_i$ is the predicted concentration obtained by the LIBS method developed in this study.

Results and discussion

Study and selection of the LIBS system operating conditions

To optimize the process of obtaining the emission signals from samples using the LIBS system previously described, a Doehlert design was employed because, among its other advantages, it is
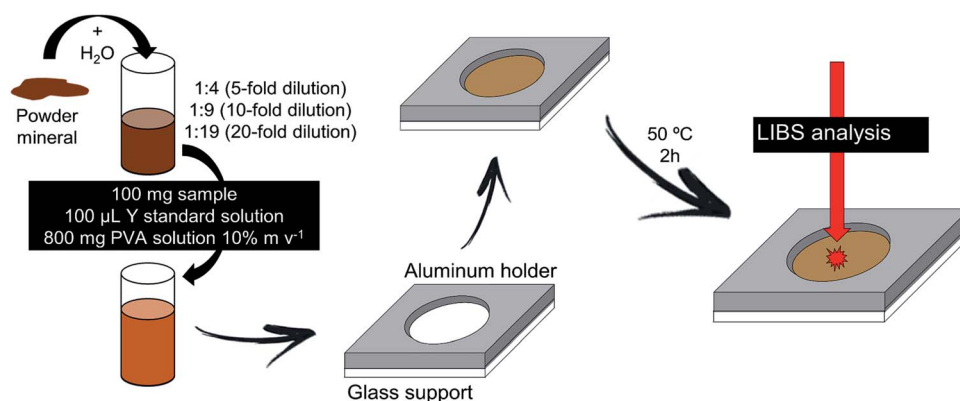

Fig. 1 Pictorial description of the sample preparation method used: slurry preparation and mixture with PVA and internal standard solutions, transference to an aluminum holder, drying and analyses processes.
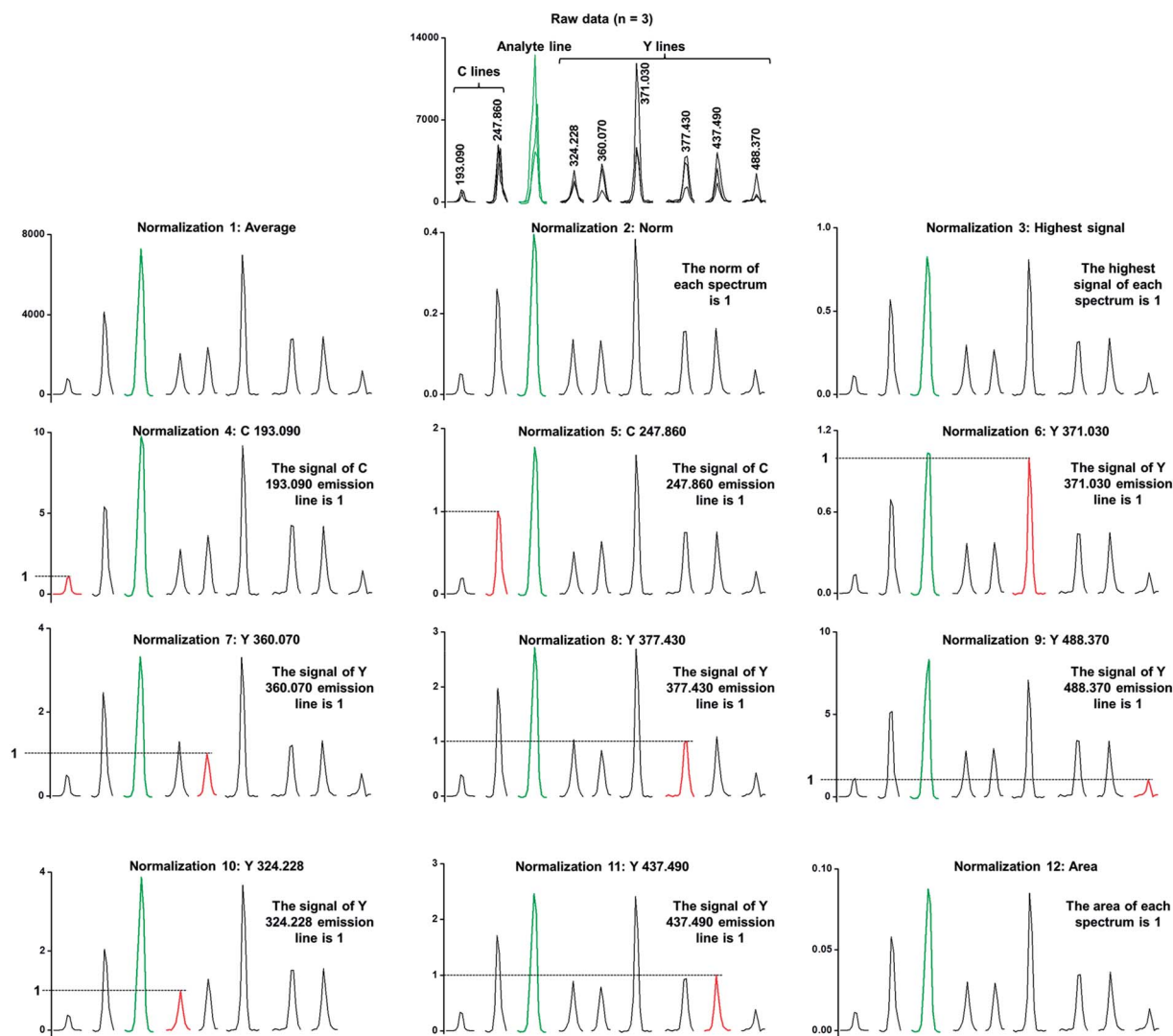
Fig. 2 Pictorial description of normalization processes applied in this study (adapted from Castro *et al.*[21]): raw data with three replicates and normalizations applied.

the most efficient in terms of the number of coefficients for the model estimated and the number of experiments performed.[22] To avoid saturation of the LIBS system detector and/or no detection of some signals, an appropriate sample was used in the optimization. In Table 1, the operating conditions for all the experiments performed are detailed, *i.e.*, the thirteen experiments that correspond to the selected experimental design plus two replicates of experiment number 1 (Central point, CP). The desired response was the higher intensity of the signals of the elements assessed (Al, Cr, Fe, Mg, Mn, and Ni). In addition, the SBRs of the analyte signals were also considered to determine the optimized operating parameters. Except for two lines of Mg (279.553 and 280.270 nm), for which saturation of the detector was observed, most signals were adequately measured and further assessed. As expected, the intensity of the emission lines of interest in the experiments with a delay time of 0 μs was higher than that in any other experiment, but the background under this condition was also high. Therefore, in the initial set

of experiments, the results for experiments 8 and 10 with a delay time of 0 μs were not considered.

Finally, a desirability function[23,24] was used to create a global model where the operating conditions that produced the best signal would be highlighted. The desirability function was created using the area under the peak as the analytical signal. The variation in the desirability function regarding the spot size variable was not important. For this reason, a contour plot is shown in Fig. 3 with the theoretical model (equation in the graph) of the desirability function considering only the laser pulse energy (V_1) and delay time (V_2) variables. The chosen operating conditions were a laser pulse energy of 60 mJ, a delay time of 0.6 μs, and a spot size of 100 μm. The predicted *D* value in this condition is around 0.4.

Study and selection of the internal standard

In the first step, Y, Sc and Bi at a concentration of 1.000 mg g^{-1} (stock solution) were assessed as internal standards. After the

Table 1 Doehlert design used to determine the best LIBS operating conditions for the experiments[a]

Experiment	Laser pulse energy		Delay time		Spot size	
	Coded	Real (mJ)	Coded	Real (μs)	Coded	Real (μm)
1 (CP)	0	55	0	1	0	100
2 (CP)	0	55	0	1	0	100
3 (CP)	0	55	0	1	0	100
4	1	80	0	1	0	100
5	0.5	68	0.866	2	0	100
6	0.5	68	0.289	1.33	0.817	150
7	−1	30	0	1	0	100
8	−0.5	43	−0.866	0	0	100
9	−0.5	43	−0.289	0.66	−0.817	50
10	0.5	68	−0.866	0	0	100
11	0.5	68	−0.289	0.66	−0.817	50
12	−0.5	43	0.866	2	0	100
13	0	55	0.577	1.66	−0.817	50
14	−0.5	43	0.289	1.33	0.817	150
15	0	55	−0.577	0.33	0.817	150

[a] CP: central point.

$$D = 0.214 + 0.218v_1 - 0.326v_2 + 0.215 v_2^2$$
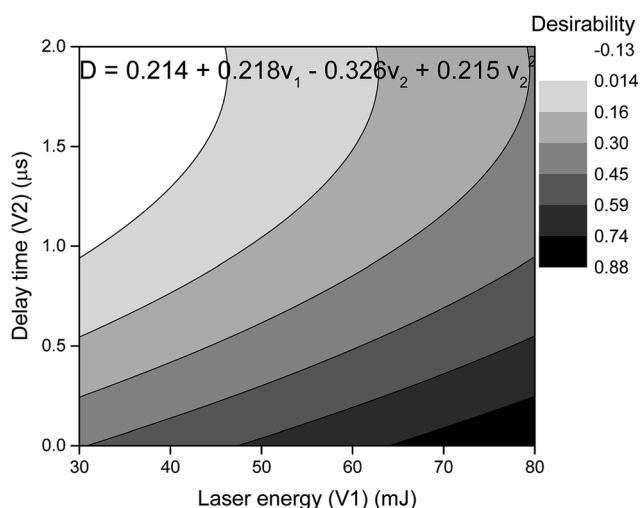
Fig. 3 Contour plot of the desirability model (D) as a function of delay time (V_2) and laser pulse energy (V_1) to reach the optimal operating conditions in the LIBS analysis of minerals.

addition of the standards to the mixture, the approximate concentration was 0.1 mg g^{-1}. As known,[25–27] the main purpose of adding known concentrations of Y, Sc and Bi to samples is to reduce the high point-by-point fluctuations normally found in LIBS spectra and to normalize the emission signals of the elements of interest using the emission signals of Y, Sc and Bi. The evaluation was made by comparing the relative standard deviation (RSD) of the non-normalized emission signal with the RSD of the emission signal normalized by each of the normalization factors used in this study. In this experiment, the same sample was prepared 3 times, each time with a different internal standard element. Since only the highest emission line for Y, Sc and Bi was assessed, 9 different spectra were generated (the
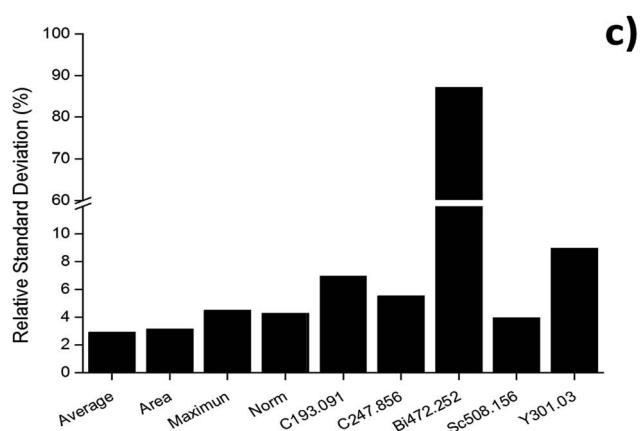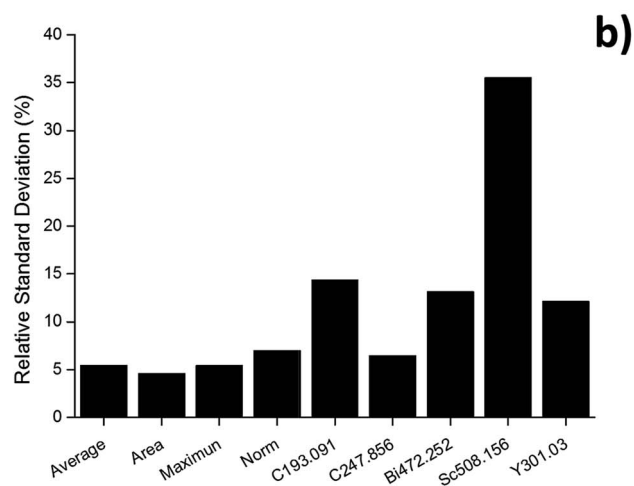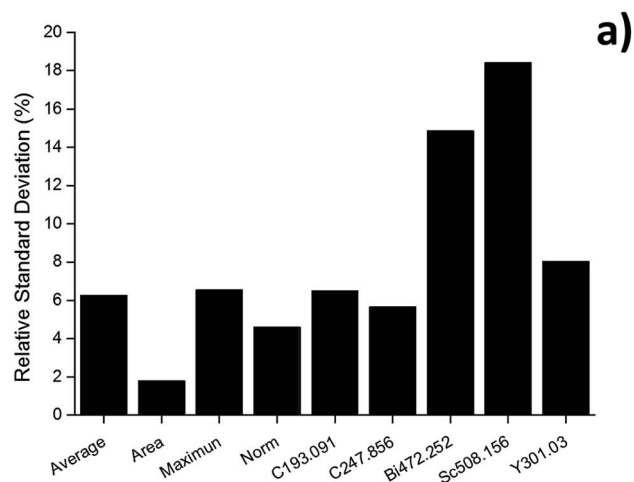
Fig. 4 Reproducibility of the emission signal of Ni estimated by the relative standard deviation (RSD) of the non-normalized signal (average) and signal normalized by the area, maximum peak height (maximum), norm, carbon emission lines (193.090 and 247.860 nm) and Y (371.030 nm), Sc (508.156 nm) and Bi (472.252 nm) lines. Subfigures (a–c) correspond to three replicates prepared from the same mineral sample.

average; the average normalized by the norm, area and peak height; the average normalized by the carbon emission lines at 193.090 and 247.860 nm; and the three spectra normalized by the Y, Sc and Bi emission lines). In Fig. 4a–c, the RSDs calculated for the 229.714 nm emission signal of Ni, which are used as an example, are shown. The RSDs for the emission signal of Ni normalized by the emission signals of Bi and Sc were, generally, higher and more varied among the studied samples than the RSDs for the analyte signal normalized by the Y signal, which excluded their use as internal standards. Therefore, Y was chosen as the best internal standard element, and more lines of Y were introduced for the normalization of the analyte signals, as mentioned in the section "LIBS data treatment" (see also details in Fig. 2).

Calibration strategy

The first calibration strategy employed was to directly correlate the reference concentrations with the corresponding areas calculated from the emission signal of each element studied in all the samples (thirty-three mineral samples and two certified reference materials). In this way, univariate models were obtained. Then, these models were used to predict the concentration in all the samples. This first step was crucial to figure out the best emission line among the ten lines proposed for each element in the TruLIBS® database and, also, to select the best normalization for the signal. In Table 2, all the emission lines

assessed as well as the correlation coefficient (R^2), slope (a), intercept (b), and SEC corresponding to the best normalization and sample dilution are shown. In the light of this information, the selected lines for further evaluation were: 396.152 nm for Al, 284.325 nm for Cr, 259.940 nm for Fe, 280.270 nm for Mg, 403.076, 403.307 and 403.449 nm for Mn, and 229.714 nm for Ni. For Mn, the three lines described were used as one due to instrumental limitation to resolve them. Among the assessed lines, a few were severely affected by spectral interferences, so it was not possible to evaluate them, and some normalizations were not effective. Normalizations by area, norm and the highest signal (see details in Fig. 2) presented the best results (the lowest error values).

Thereafter, 80% of the total samples were used as the calibration set, and the remaining 20% were used as the validation set. In this second step, each element was treated separately, and only the emission lines mentioned above were considered. Because the concentration range of each element in the samples varied, three different dilutions were made to minimize this influence and to investigate if, in the end, the same results would be observed if the dilution factor was taken into consideration.

In Fig. 5, the ICP OES reference concentrations are plotted on the X axis *versus* the concentrations found using the proposed LIBS method on the Y axis. Since this is a comparison between the reference and found concentrations determined by

Table 2 Correlation coefficient (R^2), slope (a), intercept (b), and standard error of calibration (SEC) for the initial assessment

Al: average normalized by the area; 10-fold dilution					Cr: average normalized by the norm; 10-fold dilution					Fe: average normalized by the height; 5-fold dilution				
Emission lines (nm)	R^2	A	b	SEC (%)	Emission lines (nm)	R^2	a	b	SEC (%)	Emission lines (nm)	R^2	a	b	SEC (%)
394.400	0.85	0.80	1.07	1.17	283.563	0.90	0.97	0.05	0.27	274.948	0.92	1.03	−1.39	7.23
396.152[a]	0.84	0.77	1.20	1.15	359.349	0.92	0.92	0.13	0.23	275.573	0.94	1.03	−1.39	6.30
309.271 and 309.284[b]	0.82	0.75	1.27	1.27	425.435	0.85	0.99	0.02	0.34	259.940[a]	0.96	1.03	−1.15	4.89
309.271	0.46	0.51	2.52	2.36	428.972	0.88	0.99	0.01	0.30	273.955	0.92	1.03	−1.38	7.13
					284.325[a]	0.93	0.98	0.02	0.22	263.132	0.92	1.03	−1.07	7.00
					520.604 and 520.654[b]	0.84	1.02	−0.03	0.36	274.320	0.92	1.04	−1.77	7.23

Mg: average normalized by the area; 5-fold dilution					Mn: average normalized by the area; 5-fold dilution					Ni: average normalized by the area; 10-fold dilution				
Emission lines (nm)	R^2	A	b	SEC (%)	Emission lines (nm)	R^2	a	b	SEC (%)	Emission lines (nm)	R^2	a	b	SEC (%)
279.553 and 279.799[b]	0.98	0.99	0.13	1.27	293.306, 293.93 and 294.92	−0.18	−0.35	1.03	0.77	356.637	0.11	0.19	1.12	1.20
280.270[a]	0.99	1.00	−0.01	1.24	403.076. 403.307 and 403.449[a,b]	0.89	0.99	0.00	0.16	346.165 and 345.847[b]	0.87	0.79	0.30	0.31
518.361	0.95	1.00	−0.03	2.31	356.949	0.69	0.60	0.31	0.25	351.505	0.81	0.86	0.20	0.40
517.268	0.94	1.01	−0.13	2.54	482.352	0.87	1.23	−0.17	0.23	229.714[a]	0.94	0.82	0.26	0.23
285.213	0.98	0.99	0.19	1.53										

[a] Emission lines selected to calculate the calibration models. [b] In these cases, a group of two or three emission lines of the same element was measured as only one line because the resolution of the instrument was not enough to separate each one from the rest of the group.
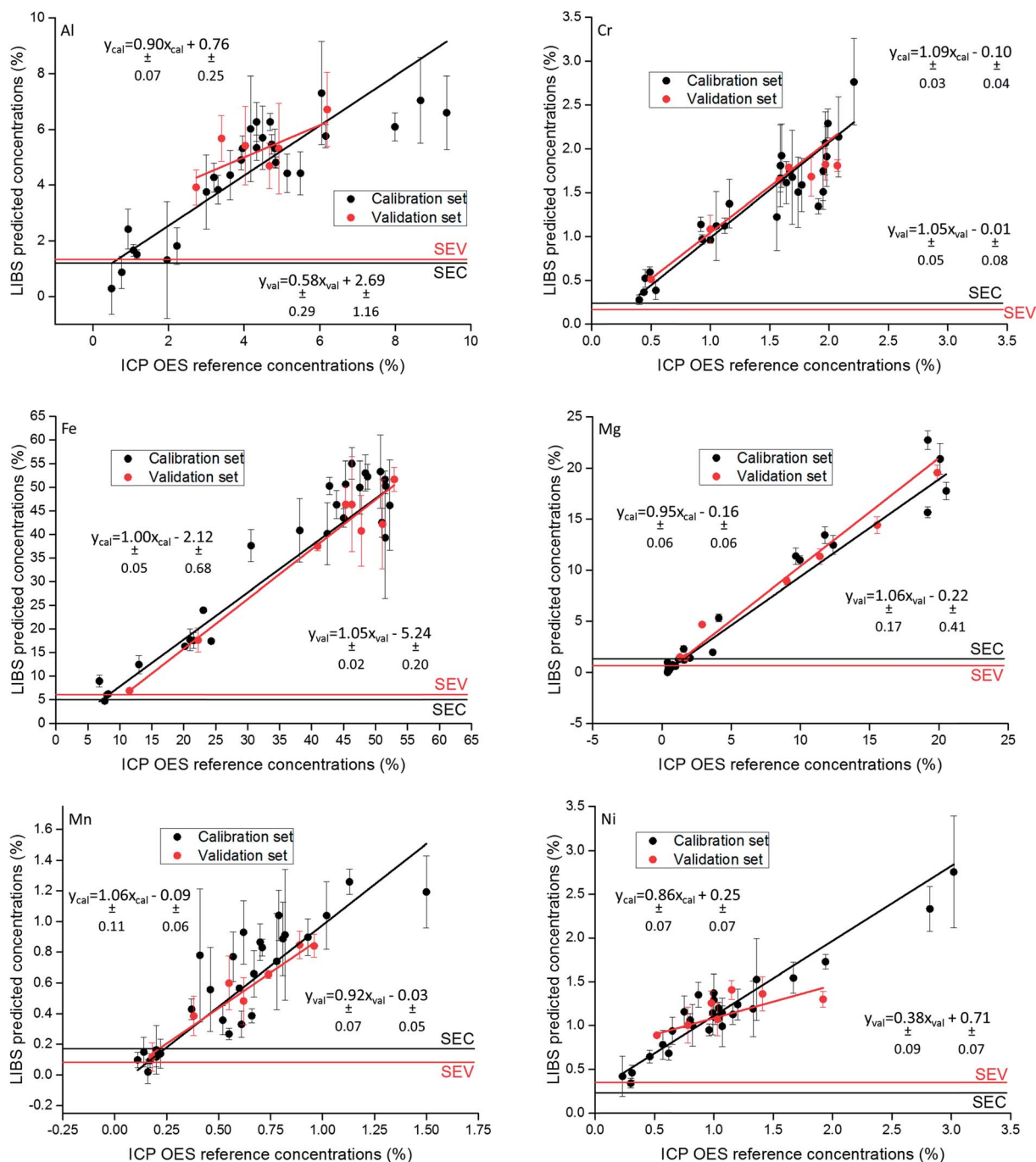
Fig. 5 Comparison of Al (396.152 nm), Cr (284.325 nm), Fe (259.940 nm), Mg (280.270 nm), Mn (403.076, 403.307 and 403.449 nm) and Ni (229.714 nm) concentrations determined in the same mineral samples by the proposed LIBS method and the ICP OES method reported previously. The SEC and SEV are added as lines parallel to the X axis.

two different methods in the same samples, the best possible result is when the angular coefficient is 1 and the intercept is 0 in the regression line equation. From the equations of the regression lines of the calibration (black) and the validation (red) sets, it is possible to see that in almost all cases the values, considering the standard deviation, either cross 1 (for the angular coefficient) or 0 (for the intercept). The model provides the best results (the lower bias) for Cr, Mg and Mn because the slope and intercept of the validation set regression

lines are statistically equal to 1 and 0, respectively. For Fe and Ni, the slope is quite close to one, but a certain underestimation of the LIBS concentration was observed. Higher deviations from the reference concentrations were observed for Al. However, on average, the calibration model fits the reference concentrations well since most of the concentrations determined by LIBS are above the SEC and standard error of validation (SEV), which are represented by two lines parallel to the X axis in Fig. 5, one in black and one in red. The SEVs for

Al, Cr, Fe, Mg, Mn, and Ni were 1.34, 0.16, 6.08, 0.88, 0.09, and 0.35%, respectively.

Conclusion

The innovative sample preparation of solid powder samples applied to minerals in this study opens a range of possibilities because it makes it feasible to prepare a slurry of any type of solid sample and immobilize it in a PVA polymer film. This strategy circumvents some drawbacks, such as the non-homogeneity of samples in pellets and the high noise in LIBS spectra, while the simplicity of a minimal and environment friendly sample preparation that characterizes the LIBS analysis of solid samples is maintained. However, attention should be paid to the lower emission signals of elements at lower concentrations.

The incorporation of liquid standard solutions of Y in the slurry made with the minerals presented good results for homogeneity and repeatability. However, the normalization of the signal of interest using the emission signal of the internal standard was not an improvement compared with the other normalizations assessed (area, norm and the highest signal).

Conflicts of interest

There are no conflicts to declare.

Acknowledgements

References

1 A. Segnini, A. Augusto Pereira Xavier, P. Luís Otaviani-Junior, E. Cristina Ferreira, A. Marcel Watanabe, M. Aurélio Sperança, G. Nicolodelli, P. Ribeiro Villas-Boas, P. Perondi Anchão Oliveira, D. Marcondes Bastos Pereira Milori and A. Segnini, *Am. J. Anal. Chem.*, 2014, **5**, 722–729.

2 M. D. Dyar, C. I. Fassett, S. Giguere, K. Lepore, S. Byrne, T. Boucher, C. Carey and S. Mahadevan, *Spectrochim. Acta, Part B*, 2016, **123**, 93–104.

3 B. Charfi and M. A. Harith, *Spectrochim. Acta, Part B*, 2002, **57**, 1141–1153.

4 S. C. Jantzi, V. Motto-Ros, F. Trichard, Y. Markushin, N. Melikechi and A. De Giacomo, *Spectrochim. Acta, Part B*, 2016, **115**, 52–63.

5 X. Yu, Y. Li, X. Gu, J. Bao, H. Yang and L. Sun, *Environ. Monit. Assess.*, 2014, **186**, 8969–8980.

6 E. Tognoni and G. Cristoforetti, *Opt. Laser Technol.*, 2016, **79**, 164–172.

7 D.-H. Lee, S.-C. Han, T.-H. Kim and J.-I. Yun, *Anal. Chem.*, 2011, **83**, 9456–9461.

8 E. M. Cahoon and J. R. Almirall, *Anal. Chem.*, 2012, **84**, 2239–2244.

9 F. F. Al-Adel, M. A. Dastageer, K. Gasmi and M. A. Gondal, *J. Appl. Spectrosc.*, 2013, **80**, 777–780.

10 H. Sobral, R. Sanginés and A. Trujillo-Vázquez, *Spectrochim. Acta, Part B*, 2012, **78**, 62–66.

11 Q. Lin, X. Han, J. Wang, Z. Wei, K. Liu and Y. Duan, *J. Anal. At. Spectrom.*, 2016, **31**, 1622–1630.

12 D. F. Andrade, M. A. Sperança and E. R. Pereira-Filho, *Anal. Methods*, 2017, 1–9.

13 Analytical Methods Committee, *Anal. Methods*, 2013, **5**, 2914–2915.

14 E. Abad-Peña, M. T. Larrea-Marín, M. E. Villanueva-Tagle and M. S. Pomares-Alfonso, *Talanta*, 2014, **124**, 79–88.

15 O. Coto, F. Galizia, I. Hernández, J. Marrero and E. Donati, *Hydrometallurgy*, 2008, **94**, 18–22.

16 L. Gao, *Metall. Anal.*, 2013, **2**, 51–54.

17 G. Wang, Y. Xu, H. Wang, F. Liu, C. Wu and Q. Hu, *Rock Miner. Anal.*, 2011, **5**, 572–575.

18 H. Feiding, L. Huachang and F. Xianjin, *Chin. J. Inorg. Anal. Chem.*, 2011, **2**, 39–41.

19 Y. Na, Z. Xiao-long, Z. Sheng-guo and Z. Hong-wen, *Rock Miner. Anal.*, 2015, **1**, 1–11.

20 G. X. Wang, F. Liu, G. Y. Wu, H. Wang and Y. J. Chen, *Chin. J. Spectrosc. Lab.*, 2013, **3**, 1230–1233.

21 J. P. Castro and E. R. Pereira-Filho, *J. Anal. At. Spectrom.*, 2016, **31**, 2005–2014.

22 S. L. C. Ferreira, W. N. L. Dos Santos, C. M. Quintella, B. B. Neto and J. M. Bosque-Sendra, *Talanta*, 2004, **63**, 1061–1067.

23 É. F. Batista, A. D. S. Augusto and E. R. Pereira-Filho, *Anal. Methods*, 2015, **7**, 329–335.

24 A. M. Neiva, M. A. Chagas Jacinto, M. Mello de Alencar, S. N. Esteves and E. R. Pereira-Filho, *RSC Adv.*, 2016, **6**, 104827–104838.

25 K. G. Fernandes, M. de Moraes, J. A. G. Neto, J. A. Nóbrega and P. V. Oliveira, *Analyst*, 2002, **127**, 157–162.

26 M. Grotti, E. Magi and R. Leardi, *J. Anal. At. Spectrom.*, 2003, **18**, 274–281.

27 A. P. Oliveira, J. A. G. Neto, J. A. Nóbrega and P. V. Oliveira, *Talanta*, 2004, **64**, 334–337.

32

Chapter 3 – Solder masks

3.1. Chapter Outline

This chapter presents the use of different spectroanalytical techniques for the characterization and determination of elemental content in solder mask samples. This material is used for the manufacture of PCB and it has the goal of providing a thin coating to prevent bridging, protecting the circuit from corrosion and mechanical damage, avoiding cold solder formation. Nowadays, this type of material is available for homemade manufacturers and then, it needs to be thoroughly assessed regarding their elemental content due to healthy issues and residue management. In this context, this study aims to analyze a series of elements by ICP OES and ICP-MS. LIBS technique is used on the attempt of creation of univariate calibration models for Ba content. Four samples were used, acquired from local e-commerce website. Two of them were composed of a two-component system and the other two were ready-to-use single component. The sample preparation for ICP analysis were made through microwave-assisted acid digestion. The sample preparation for LIBS technique was configured as a simply sample immobilization above a holder: the samples were weighted directly into an aluminum holder over a glass support and they were kept in an oven for 100 ℃ for 2 h and 3 additional hours on sunlight (some samples were UV-curable). Due to the low number of samples, calibration models for LIBS was not possible, but qualitative inferences were made. The presence of Mg on the spectra suggested the use of talc ($Mg_3Si_4O_{10}(OH)_2$), source of Si (also found in the spectra) which controls viscosity of the liquid solder mask before curing. Another important element is Ba, found in some samples. This element was present on the form of $BaSO_4$ used due to its properties such as electrical insulation, surface hardening, and flame-retardant action. For ICP analysis, an additional sample preparation step was needed due to the insolubility of $BaSO_4$. In this case, LIBS overcome ICP based techniques on the

34

identification of Ba. If there were a higher number of the samples, calibration models to determine Ba, Mg and other elements would be possible, showing the feasibility of the technique on this subject of research.

3.2. Determination of Elemental Content in Solder Mask Samples Used in Printed Circuit Boards Using Different Spectroanalytical Techniques
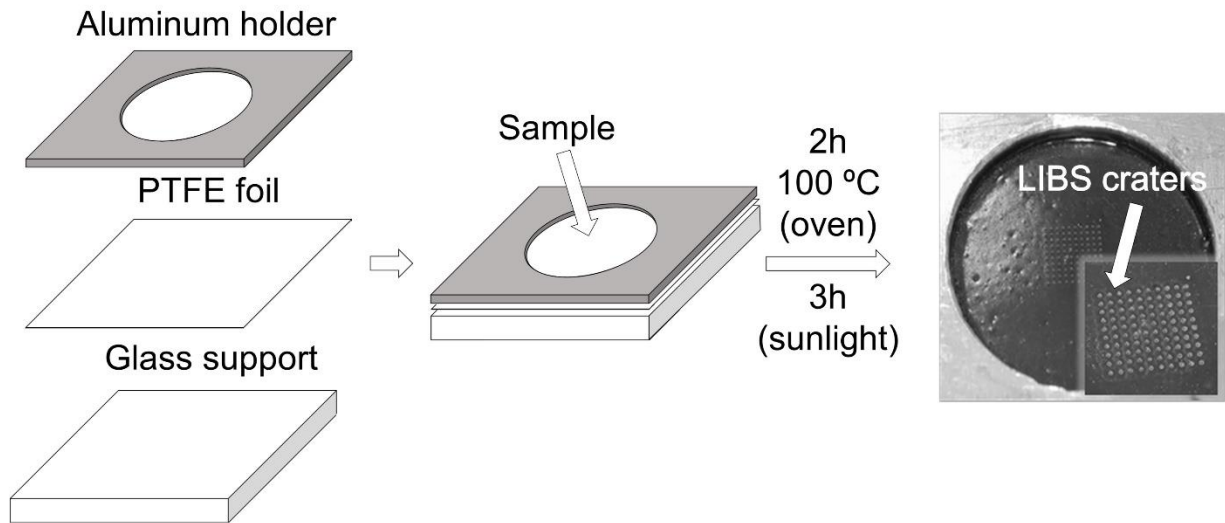

FIGURE 3.1 – Sample preparation for solder mask samples for direct LIBS analysis.

Article

Determination of Elemental Content in Solder Mask Samples Used in Printed Circuit Boards Using Different Spectroanalytical Techniques

Marco Aurelio Sperança, Alex Virgilio,
Edenir Rodrigues Pereira-Filho, and
Francisco Wendel Batista de Aquino

Abstract

Solder masks are essential materials used in the manufacture of printed circuit boards (PCB). This material protects PCBs against several types of damage and performance failure. In this study, the capabilities of laser-induced breakdown spectroscopy (LIBS) were investigated for the direct analysis of solder masks typically commercialized for homemade PCB production, and inductively coupled plasma–optical emission spectrometry (ICP-OES) was used to obtain a chemical profile for the target analytes Al, As, Ba, Cd, Co, Cr, Cu, Fe, Hg, Mg, Mn, Ni, Pb, Sb, Sn, and Zn. Inductively coupled plasma–mass spectrometry (ICP-MS) was also employed for the determination of potentially toxic elements, such as As, Cd, Cr, Pb, and Hg. In addition to the qualitative information that may be useful for obtaining the spectral profile related to the raw materials present in solder masks formulations, LIBS was also applied for major elements (Al, Ba, Cu, Fe, Mg, and Zn) determination, but due to the low sensitivity, the obtained results were only semi-quantitative for Ba. Regarding Cd, Cr, Hg, and Pb, the samples analyzed were following the restriction of hazardous substances (RoHS) directive of the European Union.

Introduction

Solder masks are indispensable materials for printed circuit board (PCB) manufacturers. Also known as solder resist or solder stop, these products are composed of polymers with low surface energy that perform many important properties. These include: (1) providing a thin coating on the printed circuit board surface to prevent solder from bridging; (2) protecting the circuit from corrosion and mechanical damage, adjusting the amount of solder attachment; (3) avoiding cold solder formation; and (4) increasing the degree of insulation of the PCB.[1–3] Visually, the green color[1] often observed in the PCBs is a characteristic indicator of the solder mask application. However, these products can be obtained with different colors and several varnishes may be used for homemade PCB preparation. Considering their chemical composition, solder masks are complex matrices based on reactive materials with

thermally or ultraviolet (UV)-curable polymers (usually epoxies or acrylates). During its formulation, a wide range of components can be included, such as solvents (e.g., halohydrocarbon), resins, curing agents, UV-curable monomers/oligomers/binders, photoinitiators, fillers, and pigments.[2,4]

Solder masks are frequently the subject of technological studies aiming for the improvement of their properties, such as reducing viscosity and curing time, improving adhesion to the PCB surface, resistance to soldering, solder

Grupo de Análise Instrumental Aplicada (GAIA), Departamento de Química, Universidade Federal de São Carlos (UFSCar), Brazil

Corresponding author:
Francisco Wendel Batista de Aquino, Grupo de Análise Instrumental Aplicada (GAIA), Departamento de Química, Universidade Federal de São Carlos (UFSCar), PO Box 676, São Carlos, SP, 13565-905, Brazil.
Email: wendelaquino@gmail.com

joint geometry, insulation resistance, effects on electro-chemical migration, and surface characteristics.[1–3,5–9] The regulations and requirements regarding the quality parameters of solder mask products used by big PCB assemblers are often defined by technical associations, such as the Institute for Interconnecting and Packaging Electronic Circuits (IPC).[10,11]

Considering the aspects related to health issues, the allergenic potential of epoxy resins has already been reported in the literature.[12] In addition, the solder mask formulations may be also a source of potentially toxic elements As, Cd, Hg, and Pb. Despite the growing interest in raw materials used in PCB production, the solder mask inorganic composition, mainly for PCB homemade production, is underexplored in literature. Most of the studies are related to polymerization using infrared spectroscopy.[13] It is still unprecedented the use of laser-induced breakdown spectroscopy (LIBS)[14,15] for this purpose.

The quantitative analysis by LIBS is still a challenge for complex matrices considering the lack of compatible reference standards, sample heterogeneity, LIBS pulse-to-pulse signal fluctuation, and spectra complexity due to the abundance of emission lines and high concentration of some analytes. The increase of the technology involving the assembly of the LIBS instruments has helped to reduce these drawbacks; however, the scientific community seems to be going toward the improvement of the statistical and mathematical approaches on LIBS data to optimize the results provided by LIBS spectra, being the main normalization or signal standardization tool for it.[16–20]

In this study, the possibilities of LIBS for the direct analysis of solder mask commercialized for homemade PCB production were investigated. Inductively coupled plasma optical emission spectrometry (ICP-OES) was used to determine the following elements: Al, As, Ba, Cd, Co, Cr, Cu, Fe, Hg, Mg, Mn, Ni, Pb, Sb, Sn, and Zn. The LIBS signals obtained and the quantitative information from ICP-OES were combined in an attempt to obtain univariate regression models.

Considering the high sensitivity required for hazardous elements As, Cd, Cr, Pb, and Hg, inductively coupled plasma mass spectrometry (ICP-MS) was also used to obtain quantitative information. This approach is particularly relevant considering that installations for PCB homemade production (mainly in the case of hobbyists) are normally not equipped with personal safety equipment and plans for residue management.

Experimental

Samples and Reagents

Four solder mask samples were purchased from a Brazilian e-commerce website: one varnish sold as a solder mask and three regular UV-curable green solder masks. Table I shows the details of the samples used. Two of these samples (samples 2 and 3) are a two-component system (parts a and b) for mixture before the application, and the other two samples (1 and 4) are a unique "ready to use" material type. These samples were chosen because they were tagged as the best-selling products and may be widely available to customers by shipping.

Nitric acid (HNO_3) and hydrochloric acid (HCl) used for sample preparation were previously purified with the Distillacid BSB-939-IR (Berghof, Germany) and Milestone duoPur (Sorisole, Italy) sub-boiling systems, respectively. The ultrapure water (18.2 ΩM cm resistivity) used to prepare all solutions was obtained using a Milli-Q Plus Total Water System (Millipore Corp.). The multi-element standard solutions were prepared by appropriate dilution of single element stock solutions of 1000 mg L^{-1} As, Cd, Co, Cr, Hg, Ni, Pb, Sn (Qhemis, Brazil), Al, Ba, Cu, Fe, Mg, Mn, Sb, Zn (Fluka, Switzerland) in 0.67 mol L^{-1} HNO_3. The blank solution was composed by a 0.67 mol L^{-1} HNO_3.

Analytical grade EDTA-Na$_2$.2H$_2$O from Synth (Diadema–SP, Brazil) and KOH from Merck (Darmstadt, Germany) were also used to investigate the chemical composition of samples solid residues after microwave-assisted assisted digestion.

Sample Preparation

Sample digestion for ICP-OES and ICP-MS analysis were performed using a cavity microwave oven Speed Wave Four (Berghof, Germany). Sample masses of 100 mg were

Table I. Solder mask samples description.

Sample	Description	Subsample	Code	Origin
1	Alternative solder mask (varnish)	Unique material Ready to use	S1	Brazil
2	Two-component green solder mask	Part a	S2a	China
		Part b	S2b	
3	Two-component green solder mask	Part a	S3a	China
		Part b	S3b	
4	Green solder mask	Unique material Ready to use	S4	China

accurately weighed in the TFM-PTFE digestion vessels (DAK-100) followed by the addition of a 7 mL mixture of HNO_3 (65%) and HCl (37%) at a 6 : 1 ratio. The six-step heating program was as follows: (1) 5 min ramp to 160 °C; (2) 15 min plateau at 160 °C; (3) 5 min ramp to 220 °C; (4) 25 min plateau at 220 °C; (5) 25 min ramp to 50 °C; and (6) 10 min plateau at 50 °C.[21]

The cooled digests were quantitatively transferred to 50 mL polyethylene tubes and the volume was made up to 50 g with deionized water. All sample solutions were paper filtered (C41; 7–12 μm particle retention; Unifil, Germany) before the analysis.

The final solutions were twofold and 200-fold diluted with a 0.67 mol L^{-1} HNO_3 to reach the appropriate acidity for ICP-OES and ICP-MS analysis, respectively. For the ICP-MS, the dilution was much higher than for ICP-OES due to the carbon content in the samples that can jeopardize the method sensitivity.

The samples S1, S2b, and S4 were completely digested, but samples S2a, S3a, and S3b presented a white solid residue in suspension. The solid residues collected after centrifugation and filtration steps were submitted to a complementary preparation procedure: (1) washing of the residues with a 5 mL aliquot of 1% HNO_3 followed by two 15 mL aliquots of water; and (2) addition of 5 mL of EDTA–Na_2 0.18 mol L^{-1} in KOH pH = 12 and heat at 80 °C for 6 h.[22] The resulting solutions were filtered and diluted, and the pH was adjusted to 8.5 and analyzed using ICP-OES.

Laser-induced breakdown spectroscopy experiments were performed with minimum sample preparation. Sample masses of approximately 100 mg were spread on a support composed by three stacked layers of different materials. The first layer was a rectangular glass piece (45 mm width × 35 mm height × 3 mm thickness), the second was a PTFE foil (Teflon), and the top layer was an aluminum holder (45 mm width × 35 mm height × 1 mm thickness) with an internal circle of 24 mm of diameter. Figure 1 shows, from left to right, views of the sample support and a closer look of the sample after LIBS analysis, with the craters highlighted.

The samples placed in supports were left in a drying oven at 100 °C for 2 h and then left directly in sunlight for an additional 3 h.

Instruments Operational Conditions

The ICP-OES measurements were performed using an iCAP 6000 instrument (Thermo Scientific, USA) using both axial and radial viewings. The ICP-MS measurements were performed in an Agilent 7800 ICP-MS (Agilent Technologies, Japan) equipped with a collision–reaction cell pressurized with He. Argon 99.996% (White Martins-Praxair, Brazil) was used for plasma generation in both instruments. Table II shows the operating parameters of both plasma systems.

All spectra from solid samples were obtained using a J200 LIBS system (Applied Spectra, USA). This system was fully controlled (including the creation of ablation patterns) by the software Axiom 2.5 (Applied Spectra) and consisted of a nanosecond 1064 nm neodymium-doped yttrium aluminum garnet (Nd:YAG) laser (Quantel Ultra, USA) that provided up to 100 mJ of laser pulse energy with a duration of 8 ns. A six-channel charge-coupled device spectrometer with a spectral window of 186–1042 nm (12 288 emission lines and resolution in the range of 0.05–0.1 nm) was used for data acquisition. An *xyz* translational ablation chamber with a 1280–1024 CMOS color camera imaging system was used to perform the ablation pattern (Fig. 1). Although this system is assembled with the possibility of hyphenation with other techniques, such as ICP-OES or ICP-MS, it requires some modules installation that was not done in our instrument yet.

The ablation pattern consisted of an array of ten rows and ten columns (100 ablation points). For each ablation point, ten laser pulses were irradiated, resulting in an acquisition of 1000 spectra per sample through the following operational conditions: laser pulse energy of 40 mJ; repetition rate of 10 Hz; spot size of 150 μm; fluence of 226 J cm^{-2}; irradiance of 28 GW cm^{-2}; delay time of 1.0 μs;
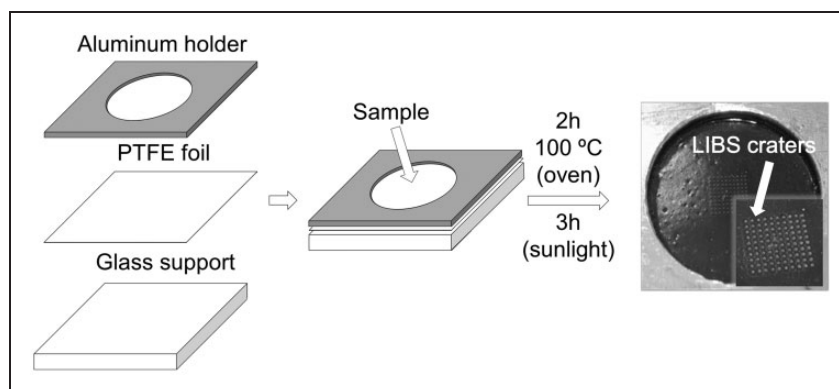
Figure 1. Views of the sample support and of a sample after LIBS analysis.

Table II. Instruments parameters for the Thermo Scientific iCAP 6000 ICP-OES and Agilent 7800 ICP-MS.

Instrument parameter	ICP-OES	ICP-MS
RF applied power (W)	1250	1550
Plasma gas flow rate (L min^{-1})	12	12
Auxiliary gas flow rate (L min^{-1})	0.5	1.8
Carrier gas flow rate (L min^{-1})	0.5	1.01
Sampling depth (mm)	–	8
Pump stabilization time (s)	5	5
Integration time (s)	15 (low); 5 (high) emission wavelengths	0.3
Nebulizer	Concentric	Concentric
Spray chamber	Cyclonic	Scott-double pass
Replicates (n)	3	3
View mode	Radial	–
Cell gas	–	4.5 mL min^{-1} He
Elements and λ (nm)—ICP-OES and m/z's—ICP-MS	Al 309.283, Ba 493.409, Cd 226.502, Co 237.862, Cr 267.716, Cu 324.754, Fe 238.204, Mg 280.270, Mn 257.610, Ni 231.604, Pb 220.353, Sb 206.833, Sn 189.989, Zn 213.856	52 (Cr), 75 (As), 114 (Cd), 202 (Hg), 208 (Pb)

and gate width of 1.05 ms. Before the analysis, a surface clean step was performed using one laser pulse (fluence 41 J cm^{-2}) at each point of the ablation pattern.

Laser-Induced Breakdown Spectroscopy Data Collection and Analyses

The emission lines related to the elements of interest were identified through Aurora software (Applied Spectra). After the spectra acquisition, the data were organized in matrices (Microsoft Excel) and data processing was performed using the Matlab software (v.R2017b, The Mathworks, Inc.) using the homemade routines "libs_treat" and "libs_par".[23]

A preliminary data inspection was carried out using the libs_treat routine (performed for each of the 1000 spectra obtained per sample) and standard deviations were calculated aiming to identify the occurrence of outliers in spectra. An outlier sample is easily observed when spectra register zeros due to some failure in the system. In this case, the standard deviation will be clearly different from the other spectra. Then, 12 normalization modes were evaluated considering several data features such as signal intensities of C emission lines, among others,[17,19] as shown in Table III.

After the normalization step, the libs_par routine was used for calculation of signal-to-background (S/B) ratio, both signal area and height of the target emission line, considering the emission line intervals that contains both the background and the signal previously established.[23] The main reason for normalizing the signals using carbon lines is that the matrix from solder masks is polymer-based, thus, behaving as a convenient inside-matrix internal standard.

Results and Discussion

Preliminary Data Inspection

Typical emission spectra (average of $n = 1000$) obtained from two traditional solder mask samples (S4 and S2a, see Table I) and from an alternative solder mask (S1, Fig. 2c) are shown in Fig. 2 (Fig. 2a and 2b, respectively).

In the spectrum from sample S4 depicted in Fig. 2a, the peaks related to Mg are the most intense. Although Mg is currently used as $Mg(OH)_2$ for flame retardancy properties in certain electrical and electronic applications, it is most likely that the source of Mg in this sample is talc ($Mg_3Si_4O_{10}(OH)_2$). This chemical compound is usually applied to solder mask formulations as a Si source, used to control the viscosity of the liquid solder mask prior to curing.[6,24,25] In this sense, as expected, Si emission signals were also observed in this spectrum and may be related to talc presence. In addition, the presence of Ca emission lines can be attributed to other fillers commonly used in solder mask formulations, such as calcium carbonate and/or calcium silicate.[25–27]

Considering the spectrum of Fig. 2b (sample S2a) the presence of Mg and Si is also observed in the formulation. However, the most remarkable characteristic of this spectrum is the number and the intensity of Ba signals. The occurrence of Ba in solder mask formulations is notably frequent and one of the most likely sources is $BaSO_4$, which is commonly incorporated in formulations as a filler due its electrical insulation, surface hardening, chemical resistance, and flame-retardant properties.[24–26,28]

After the acid digestion, it was observed that samples S2a, S3a, and S3b were not completely solubilized.

Table III. Characteristics of normalization modes applied in the raw data.

Normalization mode	Data processing	Remarks
1	Signal average	The 1000 spectra for each sample are averaged
2	Normalized by individual norm (vector length)	Each signal is normalized by its individual norm (Euclidean norm) and then averaged
3	Normalized by area (sum of all signals)	Each signal is normalized by its individual area (sum of all signals) and then averaged
4	Normalized by individual maximum (the highest signal)	Each signal is normalized by its individual highest signal (maximum) and then averaged
5	Signal sum	The 1000 spectra for each sample are summed
6	Normalized by individual norm and summed	Each signal is normalized by its individual norm (Euclidean norm) and then summed
7	Normalized by individual area and summed	Each signal is normalized by its individual area (sum of all signals) and then summed
8	Normalized by individual maximum and summed	Each signal is normalized by its individual highest signal (maximum) and then summed
9	Normalized by carbon emission line C(I) 193.09 nm and averaged	C(I) 193.09 nm signal is used as internal standard. Then, the normalized signals are averaged
10	Normalized by carbon emission line C(I) 193.09 nm and summed	C(I) 193.09 nm signal is used as internal standard. Then, the normalized signals are summed
11	Normalized by carbon emission line C(I) 247.86 nm and averaged	C(I) 247.86 nm signal is used as internal standard. Then, the normalized signals are averaged
12	Normalized by carbon emission line C(I) 247.86 nm and summed	C(I) 247.86 nm signal is used as internal standard. Then, the normalized signals are summed

These samples were resubmitted to the same digestion procedure and the insoluble residues were analyzed by LIBS. In all emission spectra obtained (data not shown), Ba lines were detected, probably originated from $BaSO_4$ precipitate. This information corroborates with the emission lines observed in Fig. 2b.

Comparing Fig. 2a and 2b with the spectrum shown in Fig. 2c, obtained from the alternative solder mask (sample S1, varnish, see Table I), the latter is poor in metal content. Except for Na, all emission lines identified as C, CN, H, and O can be attributed to the presence of organic molecules. It can be inferred that the PCBs made with this type of material are typically homemade products and thus should have modest applications or be expected to have low quality.

Quantitative Information Acquisition Using Inductively Coupled Plasma Optical Emission Spectroscopy and Inductively Coupled Plasma Mass Spectrometry

Tables IV and V show the results obtained for ICP-OES (Table IV) and ICP-MS (Table V) determinations. The solubilized white powder (see Sample Preparation section) observed in samples S2a, S3a, and S3b was mainly composed of Ba. In this way, for this element, the results (Table IV) were divided into three: soluble Ba content (Ba^a); Ba content obtained after solid residue solubilization

(Ba^b); and total Ba content ($Ba^c = Ba^a + Ba^b$). Ba total concentration varied from <limit of detection (LOD) to 17%. Co was found in only one sample (S2a) and Ni was not detected in any sample.

The Mg concentration in sample S4 was 1.7% w/w and this amount is not compatible with $Mg(OH)_2$, since this compound is typically presented in concentrations > 20% w/w when used as flame retardant.[28,29]

Regarding ICP-MS (Table V), Pb was detected in four samples and Hg was not detected. In general, the toxic elements concentration varied from <LOD up to 21.0 mg kg^{-1} for Pb in sample S3b.

Proposition of Linear Regression Models

After chemical inspection and quantitative information acquisition, linear regression models were proposed combining the signals obtained by LIBS and the quantitative information obtained using ICP-OES. In this case, it is necessary to select emission lines free of interference. Al, Ba, Cu, Fe, Mg, and Zn were the elements preliminary evaluated and Fig. 3 shows the signal peak profiles for the emission lines selected after the application of the most appropriate normalization mode (Fig. 3a–f, respectively). Figure 3 also shows the 3× noise (dotted line) for each spectral fragment selected. The noise values were calculated considering the surrounds emission lines for each
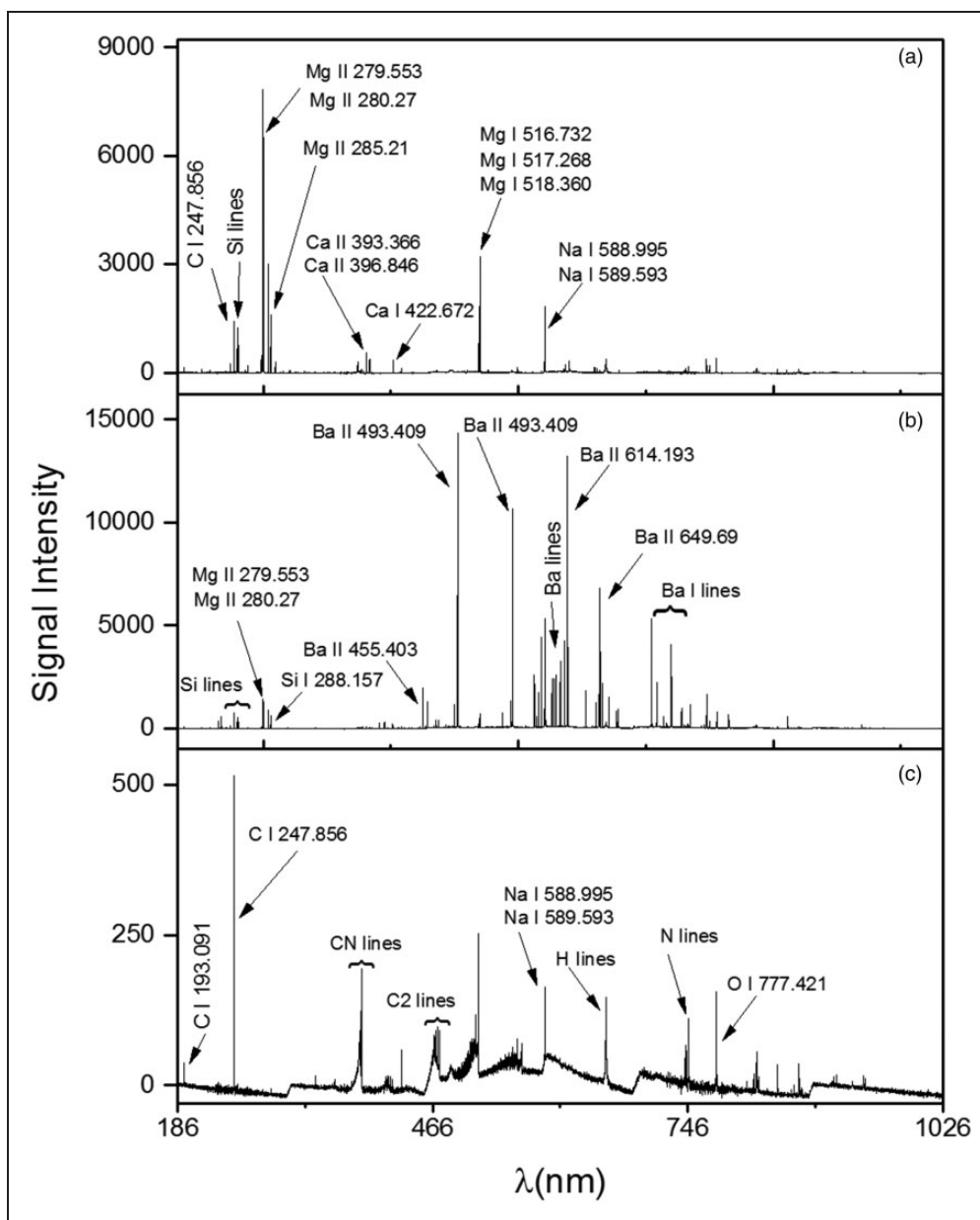
Figure 2. (a, b) Typical LIBS spectra obtained from two traditional solder masks (S4 and S2a, respectively) and (c) an alternative solder mask (varnish, S1) sample.

element. Regarding Al (Fig. 3a), samples S1, S2a, S2b, S3a, and S3b presented signal lower than the $3\times$ noise. The only exception was sample S4 that presented an Al concentration of 0.250 % (see Table IV). For Ba (Fig. 3b) only samples S2a, S3a, and S3b presented analytical signals higher than the $3\times$ noise. These samples also present Ba concentrations in percentage level (Table IV). Copper, Fe, and Mg (Fig. 3c–e, respectively) presented similar behavior, where few samples (in the case of Fe, only one sample) presented analytical signals higher than the $3\times$ noise. Zinc, as observed for Al, also presented the worst results with analytical signals in the same magnitude of the $3\times$ noise.

In this case, only for Ba, a linear model was proposed. This analyte and the related emission line was chosen based on concentration values determined by ICP-OES (Table IV) and considering the normalized results applied to the five most intense emission lines according to the Aurora software database.

The proposed linear regression model for Ba using the samples and its reference values was applied in the same samples in order to perform an internal validation, and a good concordance between the predicted and reference values was obtained for three samples (S2a, S3a, and S3b) and the recoveries varied from 97% for sample S3b to 104%

Table IV. Analyte concentrations (in mg kg^{-1}) determined in microwave-assisted digested solder mask samples (mean $\pm$ standard deviation, $n = 3$) using ICP-OES.

| Analytes | Samples | | | | | | LOD (mg kg^{-1}) |
	S1	S2a	S2b	S3a	S3b	S4	
Al	<LOD	244 ± 16	<LOD	40 ± 6	<LOD	0.250[d] ± 0.002	11
Ba[a]	<LOD	1.90[d] ± 0.03	<LOD	2.1[d] ± 0.2	2.1[d] ± 0.4	17 ± 4	2
Ba[b]	na	14.9[d] ± 0.4	na	14[d] ± 1	15[d] ± 1	na	–
Ba[c]	<LOD	16.8[d] ± 0.4	<LOD	16[d] ± 1	17[d] ± 1	17 ± 4	–
Co	<LOD	19 ± 1	<LOD	<LOD	<LOD	<LOD	14
Cu	<LOD	4.0 ± 0.4	0.27[d] ± 0.01	414 ± 5	3.90 ± 0.02	415 ± 5	2
Fe	61 ± 1	35.0 ± 0.2	87.0 ± 0.3	<LOD	56 ± 1	950 ± 3	3
Mg	<LOD	0.20[d] ± 0.01	<LOD	49 ± 2	11.0 ± 0.04	1.70[d] ± 0.05	0.3
Mn	<LOD	2.5 ± 0.2	<LOD	0.40 ± 0.01	<LOD	40 ± 1	0.4
Ni	<LOD	<LOD	<LOD	<LOD	<LOD	<LOD	3
Sb	<LOD	18 ± 1	<LOD	<LOD	53 ± 3	<LOD	9
Sn	7.1 ± 0.1	15 ± 8	29 ± 1	<LOD	85 ± 1	14 ± 1	6
Zn	6 ± 2	40 ± 17	1.40 ± 0.03	5.9 ± 0.1	22.0 ± 0.2	<LOD	0.6

[a]Ba concentration obtained from liquid phase after of microwave oven-digested material.
[b]Ba concentration obtained from dissolution of residue of microwave oven digestion with EDTA-Na$_2$ 0.18 mol L^{-1} in KOH.
[c]Ba total concentration.
[d]Values in % amounts.
na, not analyzed (without residue of sample after digestion by microwave oven).

Table V. Analyte concentrations (in mg kg^{-1}) determined in microwave-assisted digested solder mask samples (mean $\pm$ standard deviation, $n = 3$) using ICP-MS.

| Analytes | Samples | | | | | | LOD |
	S1	S2a	S2b	S3a	S3b	S4	
As	<LOD	<LOD	<LOD	<LOD	<LOD	15.0 ± 0.3	6
Cd	<LOD	7 ± 1	<LOD	<LOD	6.3 ± 0.6	1.4 ± 0.3	1
Cr	<LOD	14 ± 3	<LOD	<LOD	<LOD	1.7 ± 0.6	1
Hg	<LOD	<LOD	<LOD	<LOD	<LOD	<LOD	6
Pb	<LOD	8 ± 2	<LOD	5.7 ± 0.4	21.0 ± 0.3	2.1 ± 0.2	1

for sample S3a. It is important to mention that the proposed calibration model is semi-quantitative because it was not possible to obtain a wide Ba concentration range.

Qualitative and Quantitative Considerations

The semi-quantitative analysis of solder mask by LIBS can provide valuable information about the solder mask composition, which may be related to the raw materials used in its formulation (e.g., the Mg content) and provide information regarding the composition of materials that require extensive sample preparation for routine analysis using ICP-OES and ICP-MS. The case of barium sulfate present in samples S2a, S3a, and S3b is a clear example. Because BaSO$_4$ is practically insoluble in water (it is possible to dissolve around 500 µg in 100 mL of water, K$_{sp}$ 1.0842 × 10^{-10}) and dilute acids, an additional preparation step is mandatory for its proper determination by plasma techniques.

For ICP-OES analysis of S2a, S3a, and S3b samples, Ba concentrations determined in the liquid phase after the first digestion (soluble) were 1.90%, 2.1%, and 2.1%, respectively, while Ba concentrations of 14.9%, 14%, and 15% were determined for samples subjected to the EDTA-KOH sample preparation (insoluble) for the same samples, respectively. Therefore, the total Ba content of samples S2a, S3a, and S3b are 16.8%, 16%, and 17%, respectively. In the case of the LIBS determination, the emission signals detected are related to the total Ba content. Thus, LIBS may apply as a useful tool for a quick determination of this analyte if the system is calibrated with reference values in the suitable range.
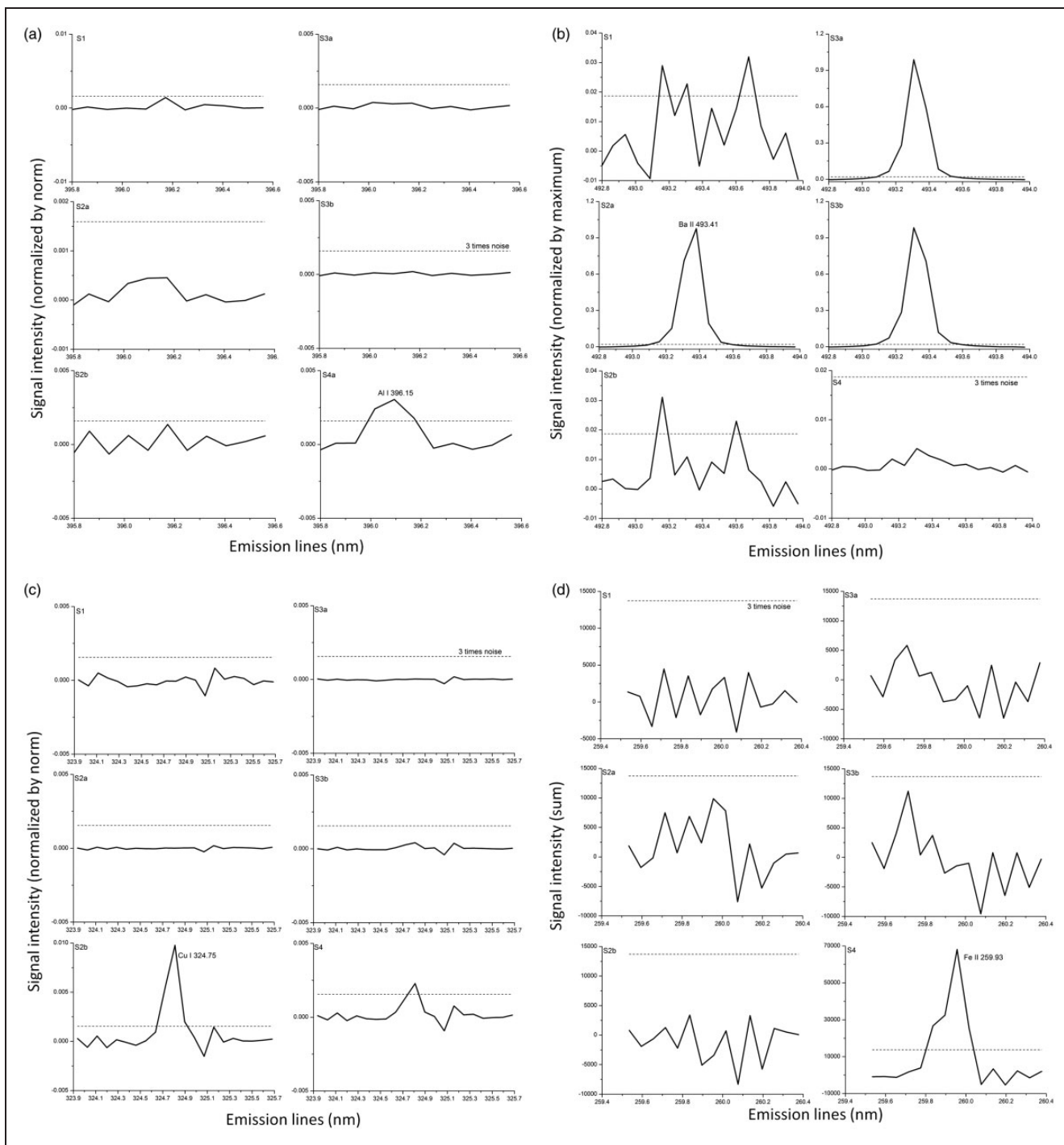
Figure 3. Signal peak profiles for the emission lines selected for (a) Al, (b) Ba, (c) Cu, (d) Fe, (e) Mg, and (f) Zn used to calculate the univariate regression models. The horizontal dotted line in each figure represents $3\times$ noise.

A further issue that hampers the LIBS quantifications is related to the severe matrix effects that this technique is prone. Aiming to minimize matrix effects associated with the variety of solder mask formulations, the preparation of a set of standards with a mixture of the samples was also evaluated, as proposed by Harrington et al.[30] Unfortunately,

the results obtained were not satisfactory and still resulted in poor precision values that limited the models to semi-quantitative analysis.

The determination of Al, As, Ba, Cd, Co, Cr, Cu, Fe, Hg, Mg, Mn, Ni, Pb, Sb, Sn, and Zn in the solder mask samples was performed by ICP-OES and ICP-MS (Tables IV and V).
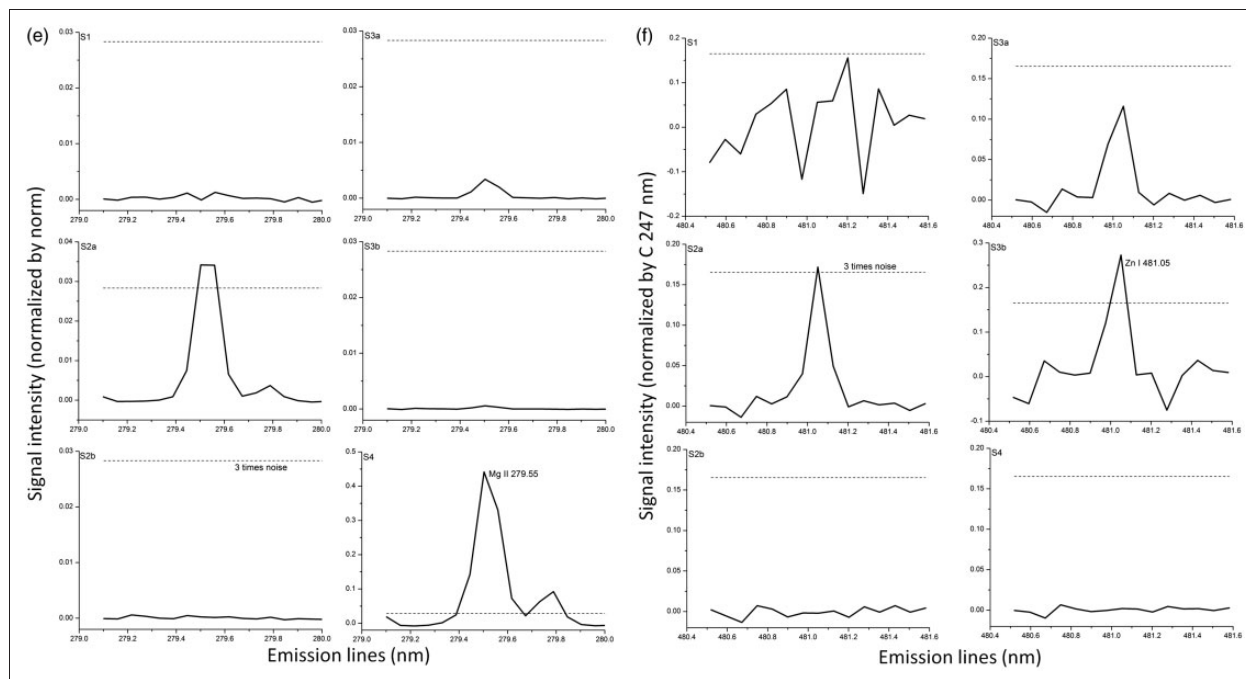
Figure 3. Continued.

The poor metallic profile for sample S1 (Fig. 2c) was predictable as observed by LIBS analysis as this sample is basically an organic varnish. Surprisingly, Sb was not detected in the samples once Sb_2O_3 is frequently used (in percent amount) to improve the flame-retardant capacity of the polybrominated diphenyl ethers commonly employed in the polymers used by the electronics equipment industry.[31,32]

As low concentrations were expected for As, Cd, Cr, Hg, and Pb in the samples, and considering the sensitivity required, these analytes were determined using ICP-MS and the results are shown in Table V. It is important to consider that toxic elements are subject to the compliance with restricted use in electrical and electronic equipment by means of the Restriction of Hazardous Substances Directive (RoHS)[33] of the European Union.

Concerning the elements controlled by RoHS, Cr, Hg, and Pb (limit of 0.1% by weight each in homogeneous materials) and Cd (0.01% by weight in homogeneous materials), all samples were below the limits established by RoHs directive (Table V). In addition, As was not found in the samples, except for S4 which presented 15.0 ± 0.3 mg/kg. As these products are primarily used for homemade activities, careful attention needs to be given to the product manipulation, waste generation, and disposal.

Despite the limits for Cd, Cr, Hg, and Pb (0.1% by weight) established by the RoHS directive, further research is mandatory to develop new procedures to produce standard materials in this concentration range to investigate LIBS as a tool for fast analysis of solder masks.

Conclusion

The association of LIBS with data normalization procedures to reduce the variability of the spectra due to sample heterogeneity, can be a useful approach for LIBS quantification methods when no solid standards are available.

The obtained results demonstrate that LIBS may be used for preliminary and semi-quantitative analysis of solder masks, including the prospecting information that can be related with raw material used in product formulation. For the plasma-based techniques, results for ICP-OES were useful to obtain quantitative information to help LIBS to propose semi-quantitative model for Ba.

Alternatively, the proposed procedure can be used in the cases where the analyte requires extensive preparation routines as the Ba originated from insoluble $BaSO_4$ for the analysis by plasma-based spectrometry techniques. Concerning the concentrations of Cr, Cd, Hg, and Pb, the samples analyzed followed the RoHS directive.

Conflict of Interest

The authors report there are no conflicts of interest.

ORCID iD

Francisco Wendel Batista de Aquino http://orcid.org/0000-0002-5218-9410.

References

1. C. Yang, Z.-G. Yang. Synthesis of Low Viscosity, Fast UV Curing Solder Resist Based on Epoxy Resin for Ink-Jet Printing". J. Appl. Polym. Sci. 2013. 129(1): 187–192.
2. R.F.H. Hang Yu, Y. Zhang, A. Wong, I.M. de Rosa, et al. "Atmospheric and Vacuum Plasma Treatments of Polymer Surfaces for Enhanced Adhesion in Microelectronics Packaging". In: K.L. Mittal, T. Ahsan, editors. Adhesion in Microelectronics, 1st ed. Hoboken, NJ: Wiley-Scrivener, 2014, pp.137–172.
3. C. Hofmeister, S. Maass, T. Fladung, B. Mayer. "Evaluation of Process Influences on Surface Chemistry of Epoxy Acrylate Based Solder Mask via XPS, ToF-SIMS and Contact Angle Measurement". Mater. Chem. Phys. 2017. 185: 129–136.
4. C.A. Camp. "Solder Masks". In: C.A. Dostal, editor. Electronic Materials Handbook: Packaging, Volume 1. Materials Park, OH: CRC Press, 1989, pp.553–560.
5. W.-H. Chen, K.-N. Chiang, S.-R. Lin. "Prediction of Liquid Formation for Solder and Non-Solder Mask Defined Array Packages". J. Electron. Packag. 2002. 124(1): 37–44.
6. T. Matynia, R. Kutyłkea, K. Bukat, B. Pieńkowska. "The Properties of Soldering Mask Hardened by Means of UV Using Acrylate and Methacrylate Oligomers". J. Appl. Polym. Sci. 1995. 55(11): 1583–1588.
7. F. Sun, S. Jiang. "Study on Properties of a Novel Photosensitive Polysiloxane Urethane Acrylate for Solder Mask". J. Appl. Polym. Sci. 2010. 116(5): 3035–3039.
8. H. Zhu, Y. Guo, W. Li, A.A. Tseng, et al. Micro-Mechanical Characterizations of Solder Mask Materials. Proceedings of the Third Electronics Packaging Technology Conference. Singapore: December 7, 2000. Pp. 148–153.
9. X. He, M.H. Azarian, M.G. Pecht. "A Study of the Effect of Solder Mask on Electrochemical Migration of Printed Circuit Board". Proceedings of the IPC Apex Conference, Volume 2. Las Vegas, NV: April 2010. Pp. 1297.
10. IPC, the Association Connecting Electronics Industries. IPC-HDBK-840 Solder Mask Handbook. Bannockburn, IL: IPC, 2006. http://www.ipc.org/TOC/IPC-HDBK-840.pdf [accessed 12 April 2018].
11. IPC, the Association Connecting Electronics Industries. IPC SM-840E. Qualification and Performance Specification of Permanent Solder Mask and Flexible Cover Materials. Bannockburn, IL: IPC, 2006. http://shop.ipc.org/IPC-SM-840E-English-D [accessed 12 April 2018].
12. K.S. Wenk, A. Ehrlich. "Allergic Contact Dermatitis from Epoxy Resin in Solder Mask Coating in an Individual Working with Printed Circuit Boards". Dermatitis. 2010. 21(5): 288–291.
13. R.W. Snyder, S.J. Fuerniss. "ATR/IR Spectroscopic Method for Following Photo-Polymer Curing". Appl. Spectrosc. 1992. 46(7): 1113–1116.
14. D.W. Hahn, N. Omenetto. "Laser-Induced Breakdown Spectroscopy (LIBS), Part II: Review of Instrumental and Methodological Approaches to Material Analysis and Applications to Different Fields". Appl. Spectrosc. 2012. 66(4): 347–419.
15. A. Ciucci, M. Corsi, V. Palleschi, S. Rastelli, et al. "New Procedure for Quantitative Elemental Analysis by Laser-Induced Plasma Spectroscopy". Appl. Spectrosc. 1999. 53(8): 960–964.

16. P. Pořízka, J. Klus, A. Hrdlička, J. Vrábel, et al. "Impact of Laser-Induced Breakdown Spectroscopy Data Normalization on Multivariate Classification Accuracy". J. Anal. At. Spectrom. 2017. 32(2): 277–288.
17. J.P. Castro, E.R. Pereira-Filho. "Twelve Different Types of Data Normalization for the Proposition of Classification, Univariate and Multivariate Regression Models for the Direct Analyses of Alloys by Laser-Induced Breakdown Spectroscopy (LIBS)". J. Anal. At. Spectrom. 2016. 31: 2005–2014.
18. N.B. Zorov, A.A. Gorbatenko, T.A. Labutin, A.M. Popov. "A Review of Normalization Techniques in Analytical Atomic Spectrometry with Laser Sampling: From Single to Multivariate Correction". Spectrochim. Acta B Atom. Spectros. 2010. 65(8): 642–657.
19. M.A. Sperança, M.S. Pomares-Alfonso, E.R. Pereira-Filho. "Analysis of Cuban Nickeliferous Minerals by Laser-Induced Breakdown Spectroscopy (LIBS): Non-Conventional Sample Preparation of Powder Samples". Anal. Methods. 2018. 10: 533–540.
20. G. Galbács. "A Critical Review of Recent Progress in Analytical Laser-Induced Breakdown Spectroscopy". Anal. Bioanal. Chem. 2015. 407(25): 7537–7562.
21. Berghof Products and Instruments. Microwave Digestion Technology: Application Report Speedwave Four v.8.0. https://www.berghof-instruments.com/en/downloads/ [accessed 12 April 2018].
22. K. Dunn, T.F. Yen. "Dissolution of Barium Sulfate Scale Deposits by Chelating Agents". Environ. Sci. Technol. 1999. 33(16): 2821–2824.
23. D.F. Andrade, E.R. Pereira-Filho. "Direct Determination of Contaminants and Major and Minor Nutrients in Solid Fertilizers Using Laser-Induced Breakdown Spectroscopy (LIBS)". J. Agric. Food Chem. 2016. 64(41): 7890–7898.
24. M. Woolley. "Corrosives on a PCB: Finding the Source". EDN Network. 2013. https://www.edn.com/design/pc-board/4422894/Corrosives-on-a-PCB–Finding-the-source [accessed 12 April 2018].
25. A. Matsumura, K. Ishikawa. Production of Solder Masked Electric Circuit Boards. US5181984 A. Filed 1991. Issued 1993.
26. R.R. Rohloff. Solder Mask Composition. US4252888A. Filed 1980. Issued 1981.
27. J.A. Serenson Jr, S. Marongelli. "The Effect of Solder Mask and Surface Mount Adhesive Types on a PCB Manufacturing Process". Proceedings of the Technical Program (West and East), National Electronic Packaging and Production Conference, Volume 2. 1999. Pp. 731–746. http://www3.uic.com/wcms/Images.nsf/(GraphicLib)/Effect_of_Solder_Mask.PDF/$file/Effect_of_Solder_Mask.PDF [accessed 12 April 2018].
28. G. Wypych. Handbook of Fillers, 2nd ed. Toronto: ChemTec Publishing, 1999.
29. R. Gul, A. Islam, T. Yasin, S. Mir. "Flame-Retardant Synergism of Sepiolite and Magnesium Hydroxide in a Linear Low-Density Polyethylene Composite". J. Appl. Polym. Sci. 2011. 121(5): 2772–2777.
30. P.B. de Harrington, E. Kolbrich, J. Cline. "Experimental Design and Multiplexed Modeling Using Titrimetry and Spreadsheets". J. Chem. Educ. 2002. 79(7): 863.
31. F.W.B. Aquino, C.M. Paranhos, E.R. Pereira-Filho. "Method for the Production of Acrylonitrile–Butadiene–Styrene (ABS) and Polycarbonate (PC)/ABS Standards for Direct Sb Determination in Plastics from e-Waste Using Laser-Induced Breakdown Spectroscopy". J. Anal. At. Spectrom. 2016. 31: 1228–1233.
32. R. Taurino, M. Cannio, T. Mafredini, P. Pozzi. "An Efficient and Fast Analytical Procedure for the Bromine Determination in Waste Electrical and Electronic Equipment Plastics". Environ. Technol. 2014. 35(24): 3147–3152.
33. European Commission. "Directive 2011/65/EU of the European Parliament and of the Council of 8 June 2011 on the Restriction of the Use of Certain Hazardous Substances in Electrical and Electronic Equipment". Off. J. Eur. Union. 2011. 54: 88–110.

Chapter 4 – Sunscreen

4.1. Chapter Outline

In this chapter, a study for determination of Ti on sunscreen will be presented. The Ti on sunscreen is on TiO_2 form, and it is a physical filter of UV radiation, scattering, reflecting and absorbing this radiation. Its concentration on sunscreen is directly correlated with the SPF (sun protection factor). The attention for this compound is increasing considerably due to the organic filters' alternative (e.g. oxybenzone) are correlated to undesired effects on the sea nature. For this analytical problem, LIBS technique was assessed as a possibility for determination of Ti on sunscreen. Five samples of sunscreen of 30 and 70 SPF from 3 different brands were analyzed by ICP OES and their reference values were obtained after hot block digestion for 4h and use of HNO_3 and HF. The sample preparation consisted on diluting the sunscreen on water (1:4) and after vortex mixing, 500 mg of the diluted sample were transferred with 500 mg of PVA solution 10 % w v^{-1} on water on a 2-ml tube. This mixture was mixed vigorously and poured into an aluminum holder on a glass support for drying on an oven for 2 h on 50 ºC. Univariate and multivariate calibration strategies were tested, as well as normalization procedures for improving the analytical results. The emission lines for Ti used for univariate and MLR strategies were: 498.17 nm and 499.11 nm. For multivariate strategies (PCR and PLS) the region from the spectra used ranged from 496 to 524 nm, region that comprehends several Ti emission lines. The Ti reference concentration on the samples ranged from 0.45 to 1.58 % w w^{-1}. The best calibration strategy evaluated was MLR using normalization 1 (average of the spectra) and using the height of the Ti signal. This calibration had SECV (standard error of cross-validation) values of 0.07 % and recoveries ranging from 97-104 %. The combination of MLR and LIBS spectra was a good alternative for Ti determination on sunscreen, since its concentration is high enough for LIBS' LOD

and the sample preparation for this type of sample was easier and safer when compared with the reference method (ICP OES) utilized in this study. The calibration models retrieved excellent results, but the model needs to always be fed in order to be as embracing as it needs to be because the formulations of sunscreen have special features not covered in this model (e.g. dry touch, facial sunscreen).

4.2. Univariate and multivariate calibration strategies in combination with laser-induced breakdown spectroscopy (LIBS) to determine Ti on sunscreen: A different sample preparation procedure
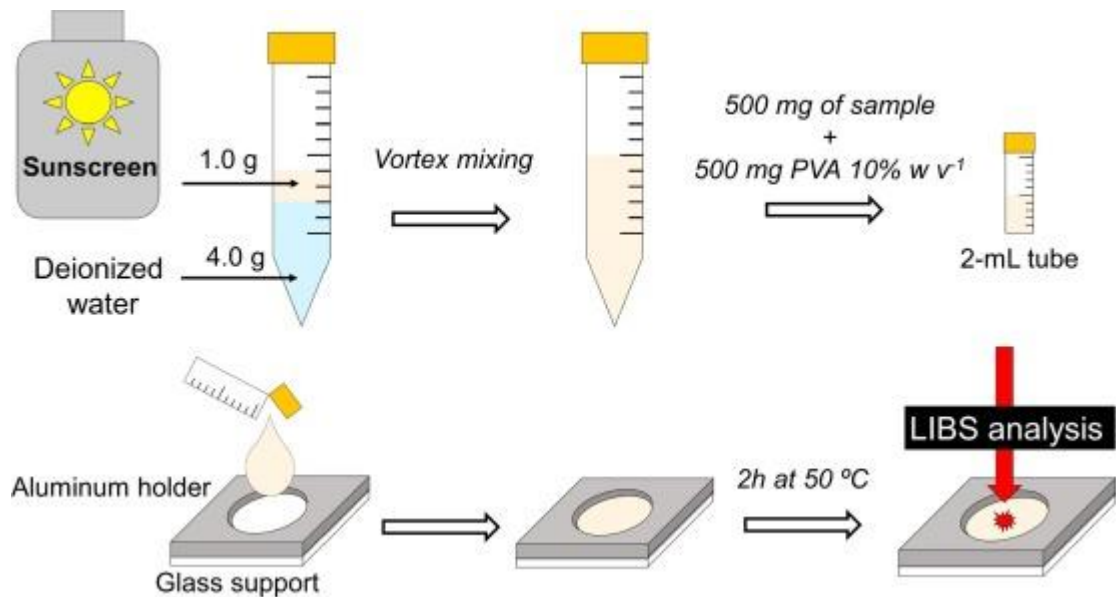

FIGURE 4.1 – Sample preparation for sunscreen samples for direct LIBS analysis.

ELSEVIER

Full length article

Univariate and multivariate calibration strategies in combination with laser-induced breakdown spectroscopy (LIBS) to determine Ti on sunscreen: A different sample preparation procedure
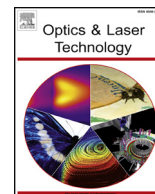
Marco Aurelio Sperança, Daniel Fernandes Andrade, Jeyne Pricylla Castro, Edenir Rodrigues Pereira-Filho*

Department of Chemistry, Federal University of São Carlos, High Way SP 310, km 235, P.O. Box 676, 13565-905, São Carlos, São Paulo, Brazil

HIGHLIGHTS

- Sunscreen immobilization in a polymer for LIBS analysis.
- Ti determination using both univariate and multivariate calibration.
- Multiple linear regression presented the lowest standard error of cross-validation.

ARTICLE INFO

ABSTRACT

Sunscreen is a cream which the intended use is to protect the human skin from ultraviolet radiation (UV) from the sun. Physical (inorganic) or chemical (organic) filters could be used to scatter the UV radiation, being TiO_2, one physical filter widely used in its formulation. To determine Ti concentrations on sunscreen, laborious and unsafe procedures must be performed involving strong acids and high temperatures in furnaces. With laser-induced breakdown spectroscopy (LIBS) the possibility of determining this element with minimal sample preparation is feasible. In this study, Ti concentration on sunscreen was determined through several calibration approaches (univariate and multivariate) with LIBS and an unusual sample preparation for sunscreen using a solution of poly(vinyl)alcohol (PVA) to immobilize the sample, converting its matrix to solid. Five samples were prepared and analyzed by inductively coupled plasma optical emission spectrometry (ICP OES) and the Ti concentration ranged from 0.45 to 1.58%. Standard errors for cross validation (SECV) and recoveries were 0.07% and 97–104% using multiple linear regression (MLR) with information from two Ti emission lines: I 498.17 nm and I 499.11 nm.

1. Introduction

Natural ultraviolet radiation (UV) have two main spectral regions: UV-A (320–400 nm) and UV-B (290–320 nm), which can cause harmful effects to human skin, such as burns and skin cancer [1–3]. Several countries issued recommendations alerting the population to not expose themselves directly to the sunlight many hours per day. On the other hand, many people inadvertently go to beach or tropical regions where the sunlight is usually strong. Tanning is one of the intended reasons where most people expose themselves to sunlight

inappropriately and end up with sunburns. Population in general day-to-day is exposed to the sunlight and need to be careful with that.

Sunscreen is a cream which intended use is dedicated to scattering the UV-radiations. For this proposal, several inorganic (physical) and/or organic (chemical) UV-filters are added in sunscreen formulations to achieve different sun protection factor (SPF) [1,4]. Generally, one of the organic filters found in its formulations is oxybenzone (benzophenone-3) which belongs to the class of aromatic ketones known as benzophenones. This molecule was approved

---

* Corresponding author.
  E-mail address: erpf@ufscar.br (E.R. Pereira-Filho).

51

for use by the Food and Drug Administration (FDA, USA) in the early 1980s, and becomes one of the most widely used organic UVA filters on sunscreen formulations. Oxybenzone works absorbing mainly on 288 nm and 350 nm peaks of UV radiation [5]. Despite of being widely used, a substantial number of important issues regarding to safety of this compound have arisen due to its toxicopathological effects on coral planulae [6]. In order to circumvent this issue, several manufacturers increase the use of TiO_2 and ZnO nanoparticles on sunscreen formulation. The concentration of these two inorganic filters on the sunscreen formulation is directly correlated with sunscreen SPF [7], moreover, it must be careful assessed in this sun care products.

Regarding to TiO_2 compound, several studies in the literature reported methods to evaluate the concentration on the sunscreen products [7], such as: flame atomic absorption spectrometry (FAAS) [8], X-ray fluorescence (XRF) spectrometry [1,9], inductively coupled plasma optical emission spectrometry (ICP OES) [10,11], ICP-mass spectrometry (ICP-MS) [12,13], and laser-induced breakdown spectroscopy (LIBS) [4].

Even with the good performance of all studies mentioned, it is undeniable that the sunscreen sample preparation is the main difficulty. This usually consists on using strong oxidizing acids on closed vessels with assistance of microwave radiation or digestor block [2,13]. Another method employed consists in laborious process using crucible, furnace at 500 °C and acids to dissolve ashes [10].

The LIBS technique is ascending the last few years as far as analysis with minimal sample preparation is concerned. This technique consists on irradiating high-energy laser pulses on a small spot of a surface to vaporize, ionize, and excite atoms. After relaxation processes, emissions of these atoms at specific emission lines are recorded by spectrometers and a spectrum is recorded [14–17]. Sample preparation for LIBS analysis is still a challenge because direct solid analysis has obstacles to be overcome such as point-by-point signal fluctuations, micro-heterogeneity, and other problems [18]. Some of these challenges can be overcome with the use of chemometrics and several strategies are employed [19–21]. Despite of calibration difficulties on LIBS analysis, some studies are employing different strategies in several materials: suspension fertilizers [22], nickeliferous minerals [23], herbs [24], and sunscreen [4].

The goal of this study is to evaluate the concentration of Ti on sunscreen samples testing different univariate and multivariate calibration strategies in combination with LIBS data set. The sunscreen samples were immobilized on a polymer (poly(vinyl alcohol), PVA) solution, converting its matrix to solid.

2. Material and methods

2.1. Reagents and samples

The reagents used throughout this study were: deionized water (18.2 ΩM cm^{-1}) produced by a Milli-Q® Plus Total Water System (Millipore Corp., Bedford, MA, USA). Nitric acid (HNO_3, 14 mol L^{-1}; Synth, Diadema, SP, Brazil) was previously purified with assistance of a sub-boiling distillation Distillacid™ BSB-939-IR (Berghof, Eningen, Germany). Hydrofluoridric acid (HF; Nuclear, Diadema, SP, Brazil) and HNO_3 were combined to mineralize the sunscreen samples for further ICP OES analysis. Boric acid (H_3BO_3, 61.83 g mol^{-1}; Mallinckrodt, Paris, France) was used to remove remaining fluorides in the digested

materials to avoid precipitation of CaF_2. A 10% w v^{-1} solution of PVA was used to immobilize the sunscreen into a polymer film. This solution was prepared using PVA Mw 89,000–98,000, 99 + % hydrolyzed (Aldrich Chemistry, St. Louis, MO, USA). Titanium stock solution containing 1000 mg L^{-1} (Merck, Darmstadt, Germany) was properly diluted in known concentrations to prepare aqueous calibration solutions for ICP OES determinations of Ti.

Five samples of sunscreen were used on this study. The samples (S1-S5) were acquired from 3 different widely known brands. S1 and S2 are from the same manufacturer (named as M1) with the SPF 30 and 70, respectively. S3 and S4 are from manufacturer M2 with the SPF 30 and 70, respectively. S5 presented the highest SPF (70) and was produced by manufacturer M3. Neither samples have special features (*e.g.* dry touch, facial sunscreen) and all described the presence of Ti on the label.

2.2. LIBS setup

The LIBS system used in this study was a J200 (Applied Spectra, Fremont, CA, USA). This instrument is a benchtop commercial system and is equipped with a 1064-nm Nd-YAG Q-switched laser with pulse duration of 8 ns. Its spectrometer consists on a 6-channel CCD with an average resolution of 70 pm and ranges from 186 to 1042 nm with 12,288 pixels. All operational parameters are controlled by Axiom software, developed by the manufacturer. The adjustable parameters are: delay time (0–2 μs), laser pulse energy (0–100 mJ), spot size (50–250 μm diameter), and laser repetition rate (1–10 Hz) while the fixed parameter is the gate width (1.05 ms). With these parameters, this equipment can reach irradiance and fluence from 0.255 GW cm^{-2} and 2 mJ cm^{-2} (250 μm spot size and 1 mJ energy) to 636.62 GW cm^{-2} and 5093 mJ cm^{-2} (50 μm spot size and 100 mJ energy), respectively, while the power ranges from 125 KW (1 mJ energy) to 12.5 MW (100 mJ energy). In this study the adjustable parameters were adapted from Sperança et al. [23]. The instrumental parameters were 75 mJ of laser pulse energy, and 100 μm of spot size. This combination provides a 955 mJ cm^{-2} fluence and 119.37 GW cm^{-2} irradiance. The delay time was 0.6 μs.

2.3. LIBS sample preparation

First, all samples were five-fold diluted in water and thoroughly homogenized with a vortex (IKA, VORTEX 1, Synth, Diadema, SP, Brazil). In this procedure, 1.000 g of the sample was accurately weighted in a 15-mL falcon tube with 4.000 g of deionized water. After that, 500 mg of this diluted sample were accurately weighted, immediately after vigorously shaking, in a 2-mL tube with 500 mg of 10% w v^{-1} PVA solution. This procedure was made in triplicate (n = 3) and the mixtures were poured into a handcraft device designed with simple components for this purpose. This device with the mixture were kept into an oven for 2 h, at 50 °C. Andrade et al. [22] and Sperança et al. [23] used the same sample preparation with slight differences. Andrade et al. [22] used the samples as received, without any handling before mixing process. Sperança et al. [23] prepared a slurry with powder mineral samples with water and, after vigorously shaking, a mass was weighted with PVA solution to make the films. The result of this process is a thin polymer film with the sunscreen encapsulated. The pictorial description of the entire procedure of sample preparation is depicted on Fig. 1.
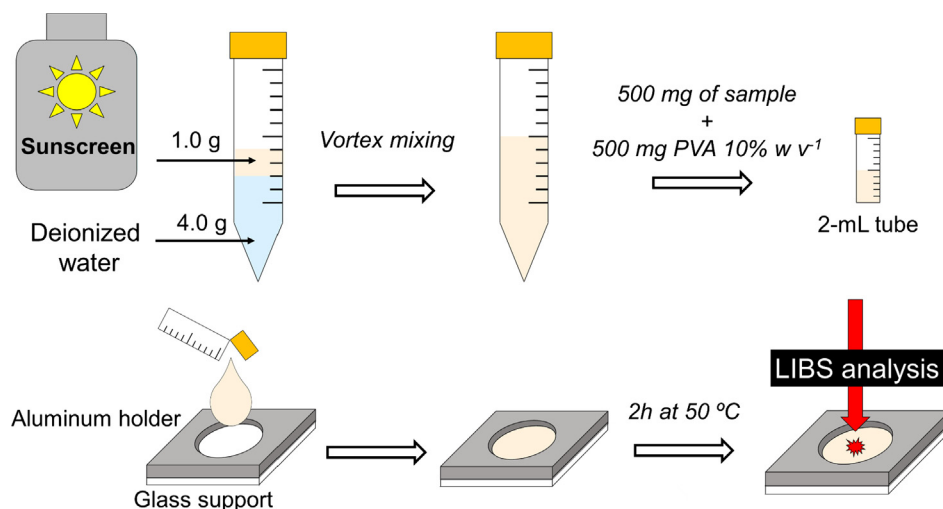
Fig. 1. Pictorial description of sunscreen sample preparation for LIBS analysis.

2.4. ICP OES instrumentation and wet digestion method

ICP OES measurements were employed to obtain Ti reference concentrations in the five samples studied. In this way, an iCAP 6000 Thermo ICP OES (Thermo Fischer Scientific, Madison, WI, USA) instrument was used. This ICP OES instrument is routinely used in our research group, and all operational parameters were already optimized [25].

For the wet digestions, a hot block digestor (Tecnal, Brazil), with 24 positions for PFA (perfluoroalkoxy, Savillex, Minnetonka, USA) closed tubes were used on the following heating program: 1 h at 50 °C and 3 h at 100 °C. This heating program was adapted from de la Calle et al. [13]. A mass of 200 mg of each sample was accurately weighted (n = 3), and added the acid mixture composed of 6 mL of HNO_3 and 2 mL of HF. After the heating program is complete, 0.5 g of boric acid was poured into the flasks. The digests were ten-fold diluted to avoid damage to ICP OES components.

2.5. Data handling and chemometric tools

All replicate from each sample were analyzed by LIBS under the conditions described on Section 2.2. Approximately 500 laser pulses were irradiated on the surface of the thin PVA film. After that, all data handling was done using MATLAB® 2017b (The Mathworks Inc., Natick, MA, USA) codes and Pirouette 4.5 (Infometrix, Bothell, WA, USA).

All spectra obtained were first normalized/standardized using a homemade MATLAB® routine that calculates 12 different modes of normalization [19]. Then, multivariate calibration models using chemometrics were calculated. The evaluation of the efficiency of each normalization and different calibration strategy employed was performed with the assistance of standard error of calibration (SEC), and recovery (trueness) of Ti.

Two chemometric approaches were used for calibration purposes: multivariate and univariate. In the case of multivariate calibration, Partial least squares (PLS), principal component regression (PCR), and multiple linear regression (MLR) were used [26,27]. Univariate strategies were also tested after selection of two Ti emission lines: Ti I 498.17 nm, and Ti I 499.11 nm.

For PLS and PCR, the entire spectra profile was initially used, and the number of latent variables (in the case of PLS) and principal components (in the case of PCR) were evaluated. For MLR, the emission lines used on the regression model were: Ti I 498.17 nm, and Ti I 499.11 nm. This region is rich of Ti emission lines and is highlighted on Fig. 2.
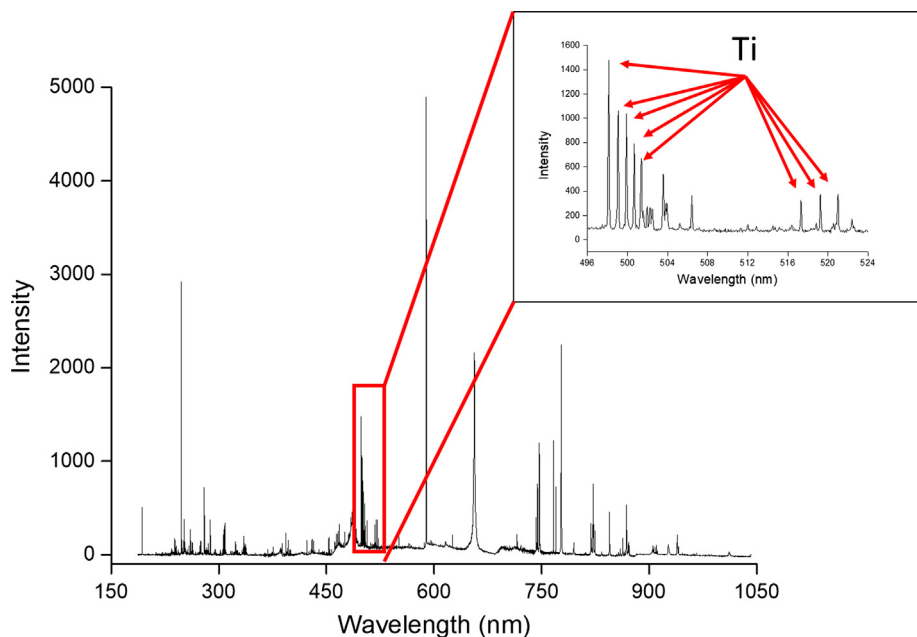

Fig. 2. Representative spectrum from sunscreen sample and region of interest with several Ti emission lines highlighted.
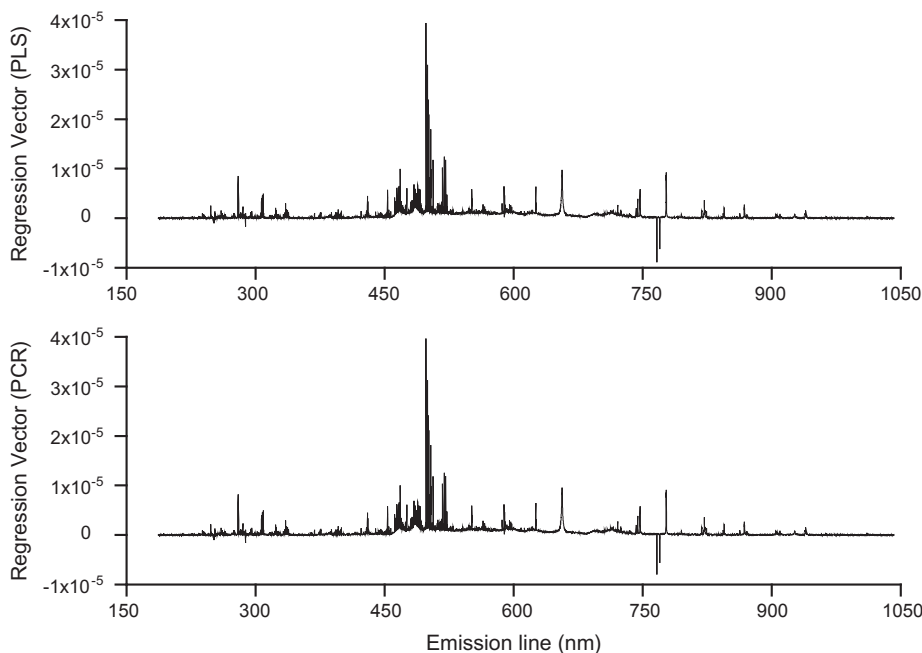
Fig. 3. Regression vectors for (a) PCR, and (b) PLS.

3. Results and discussion

3.1. Univariate calibration

All 12 normalization modes were assessed for all calibration strategies evaluated. These were: (1) average of all spectra; (2) signal normalization by the norm, then, average over all spectra; (3) signal normalization by the area, then, average over all spectra; (4) signal normalization by the highest signal, then, average over all spectra; (5) sum of all spectra; (6) signal normalization by the norm, then, sum over all spectra; (7) signal normalization by the area, then, sum over all spectra; (8) signal normalization by the highest signal, then, sum over all spectra; (9) signal normalization by C I 193.09 nm emission line, then, average over all spectra; (10) signal normalization by C I 193.09 nm emission line, then, sum over all spectra; (11) signal normalization by C I 247.85 nm emission line, then, average over all spectra; (12) signal normalization by C I 247.85 nm emission line, then, sum over all spectra. All these normalizations have been successfully employed in other studies performed by several research groups [19,28–30].

After these normalizations are performed, another homemade script (libs_par2) are used to calculate signal-to-background ratio (SBR), area, and height of a selected region of the spectra that is supposed to have the emission line of interest. With these values of area and height of this selected region, the univariate calibration models were calculated using the strategy of leave-one-out cross validation to minimize the limitation of the number of samples.

The total number of calibration models were 48, that is, 12 calibration models for each normalization for area or height of the selected region of interest (in this case, emission lines Ti I 498.17 nm, and Ti I 499.11 nm). The best normalization was chosen considering the recovery values and standard error of cross validation (SECV). In the case of univariate calibration, overall, all normalizations retrieved acceptable results, but the best ones were normalizations 2 and 6 (signal normalization by the norm, then, average and sum over the spectra, respectively) and considering the area of the region. The trueness values obtained were from 84 to 123% and SECV of 0.41%, slightly below the lower concentration (0.45%). By way of comparison, the values for recovery and SECV for only the average or the sum of all spectra were

from 89 to 126% and 0.44%, respectively. The figures of merit calculated were quite similar as far as the two lines assessed are concerned, however, the best one Ti emission line was I 498.17 nm.

3.2. Multivariate calibration

The multivariate calibration tools used in this study were MLR, PLS and PCR. These tools are now widely used, mainly PLS, and they have the capability to use entire spectrum to perform calibrations (multivariate). For MLR, two emission lines were used: Ti I 498.17 nm, and Ti I 499.11 nm. More emission lines could be used in this multivariate tool, however, one of the mathematical operation step is a matrix inversion, and this is impossible if the number of emission lines (columns) is higher than the number of the samples (rows) or a high correlation exist among variables. The twelve normalization modes were assessed for the area and height of the selected region from these lines. To obtain
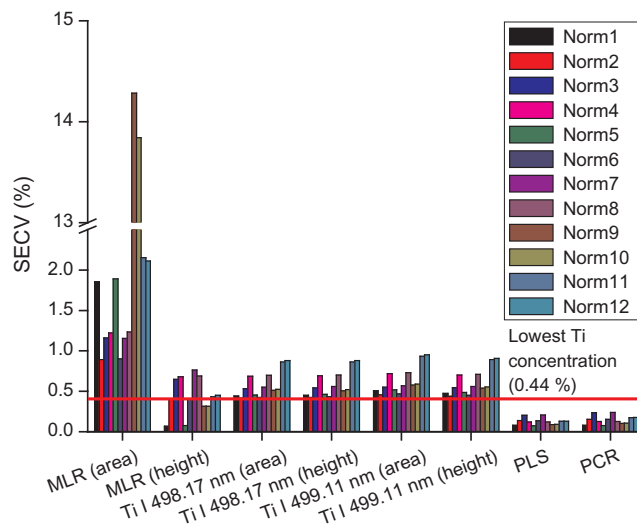

Fig. 4. Standard error of cross validation (SECV) for all normalizations and calibration strategies assessed.

651

Table 1
Reference concentration and predicted concentration from all samples analyzed in this study for all tools used with the best normalization mode, SECV, and recoveries.

	Remarks	M1S1 (%)	M1S2 (%)	M2S1 (%)	M2S2 (%)	M3S1 (%)	SECV (%)	Recoveries ranges (%)
Reference values	ICP OES determinations	0.93	1.58	0.45	0.66	0.96	–	–
Univariate Ti I 498.17 nm	Normalization 2. Area of the region	0.92	1.95	0.55	0.69	0.82	0.41	84–123
Univariate Ti I 499.11 nm	Normalization 2. Height of the region	0.94	1.97	0.54	0.71	0.79	0.45	82–125
MLR (Ti I 498.17 and Ti I 499.11 nm)	Normalization 1. Height of the region	0.95	1.64	0.47	0.65	0.94	0.07	97–104
PCR* (emission lines from 496 to 524 nm)	Normalization 1. Highlighted region from Fig. 2	0.83	1.86	0.57	0.70	0.90	0.15	89–128
PLS** (emission lines from 496 to 524 nm)	Normalization 1. Highlighted region from Fig. 2	0.83	1.88	0.57	0.70	0.90	0.16	89–128

* PCR with 1 principal component.
** PLS with 1 latent variable.

the regressions, the homemade MATLAB® script "regression2", thoroughly presented by Pereira and Pereira-Filho [31], was used. The **X** matrix was composed by 3 columns (b0, area or height from Ti I 498.17 nm, and area or height from Ti I 499.11 nm). The reference concentrations obtained from ICP OES determinations was the y vector.

PLS and PCR were performed with the entire spectra, and regression vector from these analyses are shown in Fig. 3. As can be noted several emission lines presented important regression vectors. After this, the region highlighted in Fig. 2 (only Ti emission lines) was selected to rerun the PLS and PCR calculations in order to avoid miscorrelations amongst the emission lines from other elements on Ti prediction.

The calculations were now done with the best normalization mode, that is, the one which retrieved the lower SECV values. As it is possible to see in Fig. 4, despite of PLS and PCR retrieve acceptable results in all normalization modes, the chosen one was normalization 1.

The MLR on normalization 1 and considering the height of the regions chosen from emission lines Ti I 498.17 nm and Ti I 499.17 nm showed the best SECV values and recovery values (see Table 1) for all samples.

Within the multivariate calibrations evaluated, the best results were observed for MLR. PLS and PCR showed to be less sensitive to the normalizations because all of them showed acceptable SECV values, however, MLR is chosen to be the best because it does only use Ti lines for the models, thus, there is less chance of interference problems. Using the entire spectrum to create the calibration models can bring problems, such as using an emission line from other element instead of the element of interest to correlate with the concentration of it. In fact, this was possible to observe when we compare the SECV values for PLS and PCR for normalization 1 with the entire spectra and with the highlighted region from Fig. 2. Errors increased 2-fold when only this region was used (from 0.078 and 0.080–0.16 and 0.15% for PLS and PCR, respectively).

4. Conclusion

The combination of LIBS and univariate and multivariate calibrations to determine Ti on sunscreen showed great potential, mainly due to the simple sample preparation of this type of material. It is notable that the sunscreens are an extremely variable product, furthermore, matrix effects are not always overcome with these new strategies proposed.

Within the calibrations evaluated, MLR showed the best results when compared to PLS, PCR and univariate modes. For PLS and PCR in the same normalization mode (average), the SECV and the recovery values were similar (0.16 and 0.15%, respectively).

For MLR, the recoveries ranged from 97 to 104% (Table 1) for normalization 1 and using the height instead of the area of the emission lines used, meaning that this calibration strategy could be further used on new samples. In addition, the SECV values were, at least, 2-fold lower than for PLS and PCR (next best approaches).

Only for univariate regression models the normalizations improved

the results, being the lower SECV for normalization 2, whereas for MLR, PLS and PCR, the best results were with only the average spectra. Within averaged and summed spectra, the values for SECV and recovery were very similar, being the averaged spectra slightly better than the summed spectra.

Appendix A. Supplementary material

Supplementary data associated with this article can be found, in the online version, at https://doi.org/10.1016/j.optlastec.2018.08.056.

References

[1] F.L. Melquiades, D.D. Ferreira, C.R. Appoloni, F. Lopes, A.G. Lonni, F.M. Oliveira, J.C. Duarte, Titanium dioxide determination in sunscreen by energy dispersive X-ray fluorescence methodology, Anal. Chim. Acta. 613 (2008) 135–143, https://doi.org/10.1016/j.aca.2008.02.058.

[2] G.A. Zachariadis, E. Sahanidou, Multi-element method for determination of trace elements in sunscreens by ICP-AES, J. Pharm. Biomed. Anal. 50 (2009) 342–348, https://doi.org/10.1016/j.jpba.2009.05.003.

[3] A. Samontha, J. Shiowatana, A. Siripinyanond, Particle size characterization of titanium dioxide in sunscreen products using sedimentation field-flow fractionation-inductively coupled plasma-mass spectrometry, Anal. Bioanal. Chem. 399 (2011) 973–978, https://doi.org/10.1007/s00216-010-4298-z.

[4] J. Menneveux, F. Wang, S. Lu, X. Bai, V. Motto-Ros, N. Gilon, Y. Chen, J. Yu, Direct determination of Ti content in sunscreens with laser-induced breakdown spectroscopy: Line selection method for high TiO2 nanoparticle concentration, Spectrochim, Acta - Part B At. Spectrosc. 109 (2015) 9–15, https://doi.org/10.1016/j.sab.2015.04.010.

[5] M.E. Burnett, S.Q. Wang, Current sunscreen controversies: A critical review, Photodermatol. Photoimmunol. Photomed. 27 (2011) 58–67, https://doi.org/10.1111/j.1600-0781.2011.00557.x.

[6] C.A. Downs, E. Kramarsky-Winter, R. Segal, J. Fauth, S. Knutson, O. Bronstein, F.R. Ciner, R. Jeger, Y. Lichtenfeld, C.M. Woodley, P. Pennington, K. Cadenas, A. Kushmaro, Y. Loya, Toxicopathological effects of the sunscreen UV filter, oxybenzone (Benzophenone-3), on Coral Planulae and Cultured Primary Cells and Its Environmental Contamination in Hawaii and the U.S. Virgin Islands, Arch. Environ. Contam. Toxicol. 70 (2016) 265–288, https://doi.org/10.1007/s00244-015-0227-7.

[7] A. Salvador, A. Chisvert, Sunscreen analysis A critical survey on UV filters determination, 537 (2005) 1–14. 10.1016/j.aca.2005.01.055.

[8] J.T. Mason, R. May, P. Company, S. Antonio, Quantitative determination of titanium in a commercial sunscreen formulation by atomic absorption spectrometry surface activities of barbital, phenobarbital, and pentobarbital and their interaction energies with, 69 (1980) pp. 1979–1980.

[9] V.G. Bairi, J.H. Lim, I.R. Quevedo, T.K. Mudalige, S.W. Linder, Portable X-ray fluorescence spectroscopy as a rapid screening technique for analysis of TiO2and ZnO in sunscreensSpectrochim. Acta - Part B Atmos. Spectrosc. 116 (2016) 21–27, https://doi.org/10.1016/j.sab.2015.11.008.

[10] A. Salvador, M.C. Pascual-Martí, J.R. Adell, A. Requeni, J.G. March, Analytical methodologies for atomic spectrometric determination of metallic oxides in UV

sunscreen creams, J. Pharm. Biomed. Anal. 22 (2000) 301–306, https://doi.org/10.1016/S0731-7085(99)00286-1.

[11] T. Bunhu, A. Kindness, B.S. Martincigh, Determination of titanium dioxide in commercial sunscreens by inductively coupled plasma-optical emission spectroscopy, S. Afr. J. Chem. 139–143 (2011).

[12] Y. Dan, H. Shi, C. Stephan, X. Liang, Rapid analysis of titanium dioxide nanoparticles in sunscreens using single particle inductively coupled plasma-mass spectrometry, Microchem. J. 122 (2015) 119–126, https://doi.org/10.1016/j.microc.2015.04.018.

[13] I. de la Calle, M. Menta, M. Klein, F. Séby, Screening of TiO2 and Au nanoparticles in cosmetics and determination of elemental impurities by multiple techniques (DLS, SP-ICP-MS, ICP-MS and ICP-OES), Talanta 171 (2017) 291–306, https://doi.org/10.1016/j.talanta.2017.05.002.

[14] C. Pasquine, J. Corttez, L.M.C. Silva, F.B. Gonzaga, Laser-induced breakdown spectroscopy, J. Br. Chem. Soc. 18 (2007) 463, https://doi.org/10.1366/000370210793561691.

[15] D.W. Hahn, N. Omenetto, Laser-induced breakdown spectroscopy (LIBS), part II: Review of instrumental and methodological approaches to material analysis and applications to different fields, Appl. Spectrosc. 66 (2012) 347–419, https://doi.org/10.1366/11-06574.

[16] J. Pareja, S. LÛpez, D. Jaramillo, D.W. Hahn, A. Molina, Laser ablation–laser induced breakdown spectroscopy for the measurement of total elemental concentration in soils, Appl. Opt. 52 (2013) 2470–2477, https://doi.org/10.1364/AO.52.002470.

[17] W.D. Hahn, N. Omenetto, Laser-induced breakdown spectroscopy (LIBS), Part I: review of basic diagnostics and plasma? Particle interactions: still-challenging issues within the analytical plasma community, Appl. Spectrosc. 64 (2010) 335A–366A, https://doi.org/10.1366/000370210793561691.

[18] S.C. Jantzi, V. Motto-Ros, F. Trichard, Y. Markushin, N. Melikechi, A. De Giacomo, Sample treatment and preparation for laser-induced breakdown spectroscopy, Spectrochim. Acta - Part B Atmos. Spectrosc. 115 (2016) 52–63, https://doi.org/10.1016/j.sab.2015.11.002.

[19] J.P. Castro, E.R. Pereira-Filho, Twelve different types of data normalization for the proposition of classification, univariate and multivariate regression models for the direct analyses of alloys by laser-induced breakdown spectroscopy (LIBS), J. Anal. Atmos. Spectrom. 31 (2016) 2005–2014, https://doi.org/10.1039/C6JA00224B.

[20] P. Pořízka, J. Klus, A. Hrdlička, J. Vrábel, P. Škarková, D. Prochazka, J. Novotný, K. Novotný, J. Kaiser, Impact of Laser-Induced Breakdown Spectroscopy data normalization on multivariate classification accuracy, J. Anal. Atmos. Spectrom. 32 (2017) 277–288, https://doi.org/10.1039/C6JA00322B.

[21] E. Tognoni, G. Cristoforetti, [INVITED] Signal and noise in Laser Induced Breakdown Spectroscopy: An introductory review, Opt. Laser Technol. 79 (2016) 164–172, https://doi.org/10.1016/j.optlastec.2015.12.010.

[22] D.F. Andrade, M.A. Sperança, E.R. Pereira-Filho, Different sample preparation methods for the analysis of suspension fertilizers combining LIBS and liquid-to-solid matrix conversion: determination of essential and toxic elements, Anal. Methods 9 (2017) 5156–5164, https://doi.org/10.1039/C7AY01049D.

[23] M.A. Sperança, M.S. Pomares-Alfonso, E.R. Pereira-Filho, Analysis of Cuban nckeliferous minerals by laser-induced breakdown spectroscopy (LIBS): non-conventional sample preparation of powder samples, Anal. Methods (2018) 533–540, https://doi.org/10.1039/c7ay02521a.

[24] D.F. Andrade, E.R. Pereira-Filho, P. Konieczynski, Comparison of ICP OES and LIBS analysis of medicinal herbs rich in flavonoids from Eastern Europe, J. Braz. Chem. Soc. 28 (2017) 838–847, https://doi.org/10.21577/0103-5053.20160236.

[25] É.F. Batista, A.D.S. Augusto, E.R. Pereira-Filho, Determination of Cd Co, Cr, Cu, Ni and Pb in cosmetic samples using a simple method for sample preparation, Anal. Methods 7 (2015) 329–335, https://doi.org/10.1039/C4AY02484B.

[26] R.G. Brereton, Calibration, 2003 10.1002/0470863242.ch5.

[27] D.L. Massart, B.G.M. Vandeginste, S.N. Deming, Y. Michotte, L. Kaufman (Eds.), Chemom. a Textb. Elsevier, 2003, pp. 165–189, , https://doi.org/10.1016/S0922-3487(08)70226-0.

[28] M.A. Sperança, A. Virgilio, E.R. Pereira-Filho, F.W. Batista de Aquino, Determination of elemental content in solder mask samples used in printed circuit boards using different spectroanalytical techniques, Appl. Spectrosc. (2018) 1–10, https://doi.org/10.1177/0003702818774580.

[29] V.C. Costa, F.A.C. Amorim, D.V. de Babos, E.R. Pereira-Filho, Direct determination of Ca, K, Mg, Na, P, S, Fe and Zn in bivalve mollusks by wavelength dispersive X-ray fluorescence (WDXRF) and laser-induced breakdown spectroscopy (LIBS), Food Chem. 1 (2018), https://doi.org/10.1016/j.foodchem.2018.02.016.

[30] Y. Dixit, M.P. Casado-Gavalda, R. Cama-Moncunill, X. Cama-Moncunill, M. Markiewicz-Keszycka, P.J. Cullen, C. Sullivan, Laser induced breakdown spectroscopy for quantification of sodium and potassium in minced beef: A potential technique for detecting beef kidney adulteration, Anal. Methods 9 (2017) 3314–3322, https://doi.org/10.1039/c7ay00757d.

[31] F. Pereira, E.R. Pereira-Filho, Application of free computational program in experimental design: a tutorial, Quim. Nova, accepted for publication, https://doi.org/10.21577/0100-4042.20170254.

56

Conclusions

Conclusions

In this PhD thesis it was possible to propose a sample preparation procedure for nickeliferous mineral ores and sunscreen. The procedures proposed presented some positive features as stability, safety for the operator and high analytical frequency when compared with the traditional methods based on wet digestions for further spectroanalytical determinations. The use of chemometric tools were indispensable in the data treatment and handling (exploratory analysis, normalizations, uni and multivariate analysis). For solder mask samples, only the drying process was necessary to make the liquid-to-solid matrix conversion due to their nature.

The creation of univariate models for Al, Cr, Fe, Mg, Mn, and Ni in nickeliferous minerals was possible using the sample preparation proposed in this study different from conventional solid sample preparation (pressing into pellets). The strategy employed minimized the routinely problems that are observed on the traditional solid sample preparation, that is, the pressed pellets, such as homogeneity, and roughness of the pellet (in the case of samples with high content of Si). The dilution with water could be a potential problem, but in this case, it was actually positive because some signals saturated due to the high concentration of some elements (e.g. Fe).

The analysis of solder masks by LIBS was a good alternative for qualitative determinations, mainly regarding Ba. It opens up a quantitative possibility if a larger number of samples were obtained. Due to the use of $BaSO_4$ on this type of samples, an additional step of sample preparation is necessary for total determination of Ba, making the LIBS analysis strong for this application. For the hazardous elements, such as Cr, Cd, Hg and Pb, LIBS does not presented enough sensitivity, so ICP-MS needed to be used.

This initial qualitative evaluation is important mainly because the samples is intended for homemade use.

For sunscreen analysis, the sample preparation proposed showed to be a good alternative for LIBS analysis due to the nature of the sample (viscous suspension). The reference results are reliable but the preparation for the wet-based analysis requires the use of strong and dangerous acids as HNO_3 and HF. Once again, for this application where the concentration of the element of interest is high enough, LIBS is attractive for this determination over ICP OES analysis.

Regardless the good results obtained by LIBS, this technique is not intended to replace traditional techniques, such as ICP OES and ICP-MS, but it comes to complement these traditional technique. In some cases, it is only necessary qualitative results, where LIBS is efficient, and in other cases, for quantitative results, the concentration of the elements of interest is high enough for the LIBS' sensitivity.